ISSN 1948-5204 (online)

World Journal of *Gastrointestinal Oncology*

World J Gastrointest Oncol 2019 August 15; 11(8): 567-651

Published by Baishideng Publishing Group Inc

World Journal of Gastrointestinal Oncology

Contents

Monthly Volume 11 Number 8 August 15, 2019

REVIEW

MINIREVIEWS

ORIGINAL ARTICLE

Basic Study

Retrospective Study

Contents

World Journal of Gastrointestinal Oncology

Volume 11 Number 8 August 15, 2019

ABOUT COVER

Editorial Board Member of *World Journal of Gastrointestinal Oncology*, Florin Burada, MD, PhD, Associate Professor, Department of Medical Genetics and Human Genomics Laboratory, Research Center of Gastroenterology and Hepatology, University of Medicine and Pharmacy of Craiova, Craiova 200349, Romania

AIMS AND SCOPE

World Journal of Gastrointestinal Oncology (*World J Gastrointest Oncol*, *WJGO*, online ISSN 1948-5204, DOI: 10.4251) is a peer-reviewed open access academic journal that aims to guide clinical practice and improve diagnostic and therapeutic skills of clinicians.

The *WJGO* covers topics concerning carcinogenesis, tumorigenesis, metastasis, diagnosis, prevention, prognosis, clinical manifestations, nutritional support, *etc*. The current columns of *WJGO* include editorial, frontier, field of vision, review, original articles, case report.

We encourage authors to submit their manuscripts to *WJGO*. We will give priority to manuscripts that are supported by major national and international foundations and those that are of great clinical significance.

INDEXING/ABSTRACTING

The *WJGO* is now indexed in Science Citation Index Expanded (also known as SciSearch®), PubMed, and PubMed Central. The 2019 edition of Journal Citation Reports® cites the 2018 impact factor for *WJGO* as 2.758 (5-year impact factor: 3.220), ranking *WJGO* as 52 among 84 journals in gastroenterology and hepatology (quartile in category Q3), and 131 among 229 journals in oncology (quartile in category Q3).

RESPONSIBLE EDITORS FOR THIS ISSUE

NAME OF JOURNAL
World Journal of Gastrointestinal Oncology

ISSN
ISSN 1948-5204 (online)

LAUNCH DATE
February 15, 2009

FREQUENCY
Monthly

PUBLICATION DATE
August 15, 2019

INSTRUCTIONS TO AUTHORS
https://www.wjgnet.com/bpg/gerinfo/204

GUIDELINES FOR ETHICS DOCUMENTS
https://www.wjgnet.com/bpg/GerInfo/287

GUIDELINES FOR NON-NATIVE SPEAKERS OF ENGLISH
https://www.wjgnet.com/bpg/gerinfo/240

PUBLICATION MISCONDUCT
https://www.wjgnet.com/bpg/gerinfo/208

ARTICLE PROCESSING CHARGE
https://www.wjgnet.com/bpg/gerinfo/242

STEPS FOR SUBMITTING MANUSCRIPTS
https://www.wjgnet.com/bpg/GerInfo/239

ONLINE SUBMISSION
https://www.f6publishing.com

World Journal of Gastrointestinal Oncology

Submit a Manuscript: https://www.f6publishing.com

World J Gastrointest Oncol 2019 August 15; 11(8): 599-621

DOI: 10.4251/wjgo.v11.i8.599

ISSN 1948-5204 (online)

ORIGINAL ARTICLE

Basic Study

KMT2D deficiency enhances the anti-cancer activity of L48H37 in pancreatic ductal adenocarcinoma

Si-Si Li, Wei-Liang Jiang, Wen-Qin Xiao, Kai Li, Ye-Fei Zhang, Xing-Ya Guo, Yi-Qi Dai, Qiu-Yan Zhao, Ming-Jie Jiang, Zhan-Jun Lu, Rong Wan

ORCID number: Si-Si Li (0000-0001-9375-4538); Wei-Liang Jiang (0000-0002-0304-0847); Wen-Qin Xiao (0000-0002-8621-6608); Kai Li (0000-0001-6699-2290); Ye-Fei Zhang (0000-0001-9800-9019); Xing-Ya Guo (0000-0002-2644-5126); Yi-Qi Dai (0000-0001-5802-2593); Qiu-Yan Zhao (0000-0003-2724-9052); Ming-Jie Jiang (0000-0001-8798-9904); Zhan-Jun Lu (0000-0001-6881-5810); Rong Wan (0000-0003-1824-7153).

Author contributions: Li SS and Wan R contributed equally to this work; Li SS and Wan R designed the research; Li SS, Jiang WL, Xiao WQ, Zhang YF, Guo XY and Dai YQ performed the research; Li SS, Jiang WL, Li K and Xiao WQ contributed to the analytic tools; Zhao QY, Jiang MJ and Lu ZJ provided the clinical specimen and reagents; Li SS wrote the paper.

Institutional review board statement: All patients participated in this study gave their informed consent. Institutional review board approval of our hospital was obtained for this study. Colleague Ming-Jie Jiang provided human pancreatic cancer tissue specimens in our study.

Institutional animal care and use committee statement: All animal experiments were in line with the Shanghai Jiao Tong University's Policy on the Care and Use of Laboratory Animals.

Conflict-of-interest statement: There is no conflict of interest.

Si-Si Li, Wei-Liang Jiang, Wen-Qin Xiao, Kai Li, Ye-Fei Zhang, Xing-Ya Guo, Yi-Qi Dai, Qiu-Yan Zhao, Zhan-Jun Lu, Rong Wan, Department of Gastroenterology, Shanghai General Hospital, Shanghai Jiao Tong University School of Medicine, Shanghai 201620, China

Si-Si Li, Qiu-Yan Zhao, Ming-Jie Jiang, Rong Wan, Shanghai Key Laboratory of Pancreatic Diseases, Shanghai General Hospital, Shanghai Jiao Tong University School of Medicine, Shanghai 201620, China

Corresponding author: Rong Wan, PhD, Chief Doctor, Department of Gastroenterology, Shanghai General Hospital, Shanghai Jiao Tong University School of Medicine, No. 100 Haining Road, Hongkou District, Shanghai 201620, China. doctorwanrong1970@126.com
Telephone: +86-21-63240090
Fax: +86-21-63241377

Abstract

BACKGROUND

Novel therapeutic strategies are urgently needed for patients with a delayed diagnosis of pancreatic ductal adenocarcinoma (PDAC) in order to improve their chances of survival. Recent studies have shown potent anti-neoplastic effects of curcumin and its analogues. In addition, the role of histone methyltransferases on cancer therapeutics has also been elucidated. However, the relationship between these two factors in the treatment of pancreatic cancer remains unknown. Our working hypothesis was that L48H37, a novel curcumin analog, has better efficacy in pancreatic cancer cell growth inhibition in the absence of histone-lysine N-methyltransferase 2D (KMT2D).

AIM

To determine the anti-cancer effects of L48H37 in PDAC, and the role of KMT2D on its therapeutic efficacy.

METHODS

The viability and proliferation of primary (PANC-1 and MIA PaCa-2) and metastatic (SW1990 and ASPC-1) PDAC cell lines treated with L48H37 was determined by CCK8 and colony formation assay. Apoptosis, mitochondrial membrane potential (MMP), reactive oxygen species (ROS) levels, and cell cycle profile were determined by staining the cells with Annexin-V/7-AAD, JC-1, DCFH-DA, and PI respectively, as well as flow cytometric acquisition. *In vitro* migration was assessed by the wound healing assay. The protein and mRNA

Manuscript source: Unsolicited manuscript

Received: October 22, 2018
Peer-review started: October 23, 2018
First decision: November 27, 2018
Revised: January 23, 2019
Accepted: February 27, 2019
Article in press: February 27, 2019
Published online: August 15, 2019

P-Reviewer: Azer SA, Ebrahim E, Hori T
S-Editor: Ji FF
L-Editor: Filipodia
E-Editor: Xing YX

levels of relevant factors were analyzed using Western blotting, immunofluorescence and real time-quantitative PCR. The in situ expression of KMT2D in both human PDAC and paired adjacent normal tissues was determined by immunohistochemistry. *In vivo* tumor xenografts were established by injecting nude mice with PDAC cells. Bioinformatics analyses were also conducted using gene expression databases and TCGA.

RESULTS

L48H37 inhibited the proliferation and induced apoptosis in SW1990 and ASPC-1 cells in a dose- and time-dependent manner, while also reducing MMP, increasing ROS levels, arresting cell cycle at the G2/M stages and activating the endoplasmic reticulum (ER) stress-associated protein kinase RNA-like endoplasmic reticulum kinase/eukaryotic initiation factor 2α/activating transcription factor 4 (ATF4)/CHOP signaling pathway. Knocking down ATF4 significantly upregulated KMT2D in PDAC cells, and also decreased L48H37-induced apoptosis. Furthermore, silencing KMT2D in L48H37-treated cells significantly augmented apoptosis and the ER stress pathway, indicating that KMT2D depletion is essential for the anti-neoplastic effects of L48H37. Administering L48H37 to mice bearing tumors derived from control or KMT2D-knockdown PDAC cells significantly decreased the tumor burden. We also identified several differentially expressed genes in PDAC cell lines expressing very low levels of KMT2D that were functionally categorized into the extrinsic apoptotic signaling pathway. The KMT2D high- and low-expressing PDAC patients from the TCGA database showed similar survival rates,but higher KMT2D expression was associated with poor tumor grade in clinical and pathological analyses.

CONCLUSION

L48H37 exerts a potent anti-cancer effect in PDAC, which is augmented by KMT2D deficiency.

Key words: Pancreatic neoplasms; Curcumin analog; Histone methyltransferase 2D; Therapeutic effects; Bioinformatics

Core tip: We are the first to report an anti-tumor effect of L48H37 in pancreatic cancer, and ascertain that KMT2D deficiency contributes significantly to the therapeutic effect, in part through the protein kinase RNA-like endoplasmic reticulum kinase/eukaryotic initiation factor 2α/activating transcription factor 4/CHOP signaling pathway. It is worth noting that the relationship between the KMT2D expression pattern and treatment efficacy in clinical practice has yet to be further explored.

Citation: Li SS, Jiang WL, Xiao WQ, Li K, Zhang YF, Guo XY, Dai YQ, Zhao QY, Jiang MJ, Lu ZJ, Wan R. KMT2D deficiency enhances the anti-cancer activity of L48H37 in pancreatic ductal adenocarcinoma. *World J Gastrointest Oncol* 2019; 11(8): 599-621
URL: https://www.wjgnet.com/1948-5204/full/v11/i8/599.htm
DOI: https://dx.doi.org/10.4251/wjgo.v11.i8.599

INTRODUCTION

Pancreatic ductal adenocarcinoma (PDAC) is the fourth leading cause of cancer-related deaths, with a five-year survival rate below 10%. Due to its early asymptomatic nature, only 15%-20% of the patients have the opportunity to undergo surgery after diagnosis, which renders chemotherapy and radiotherapy as the primary modes of treatment[1]. Therefore, an effective therapeutic strategy is urgently needed to improve patient survival.

PDAC has a complex etiology involving genetic and epigenetic modifications like DNA methylation and histone deacetylation, which are a reversible response to external stimuli. The histone-lysine N-methyltransferase KMT2D, also known as MLL2 or MLL4[2,3], is frequently mutated in multiple cancers[4-12], including PDAC

where it shows a mutation rate of 5%-7%[13,14]. KMT2D mutations affect the expression of chromatin-regulated genes involved in cell cycle progression, survival and epithelial-mesenchymal transition (EMT)[15-18]. Interestingly, KMT2D can act either as an oncogene or a tumor suppressor, depending on the type and stage of the tumor. In addition, studies show that variations in KMT2D expression patterns depend on the genetic background of cancer cell lines and cancer types, which has a significant impact on therapeutic response[3,10,11,17-27]. The role of KMT2D in PDAC is ambiguous, with contrasting results reported in different studies[13,15,28,29]. In this study, we analyzed the effect of KMT2D expression levels on the therapeutic efficacy of L48H37 on PDAC cells in order to determine the predictive value of KMT2D in PDAC.

L48H37 is a novel curcumin with an unsaturated monoketone structure compared to the β-diketone structure of curcumin, which increases its stability and anti-cancer effects. A recent study showed promising results with L48H37 in lung cancer cells[30]. In the present study, we observed a potent anti-neoplastic effect of L48H37 on human PDAC cells. Mechanistically, L48H37 triggered apoptosis *via* the endoplasmic reticulum (ER) stress-associated protein kinase RNA-like endoplasmic reticulum kinase (PERK)/eIF2a/activating transcription factor 4 (ATF4)/CHOP signaling pathway, which was accompanied by a slight decrease in KMT2D levels. Blocking this pathway significantly decreased apoptosis and upregulated KMT2D. Consistent with the above, KMT2D knockdown augmented the effects of L48H37 both *in vitro* and *in vivo*. Taken together, KMT2D deficiency optimizes the therapeutic effects of L48H37 in PDAC cells by activating the ER stress pathway. Our findings provide new insights into drug targets and therapeutic strategies for PDAC.

MATERIALS AND METHODS

Cell lines and patient tissue samples

The primary human PDAC cell lines PANC-1 and MIA $PaCa_2$ were cultured in high glucose DMEM (HyClone, Logan, UT, United States), while the metastatic SW1990 and ASPC-1 lines (all from American Type Culture Collection, ATCC, Manassas, VA, United States) were cultured in RPMI1640 medium (HyClone, Logan, UT, United States). Both media were supplemented with 10% heat-inactivated FBS (HyClone, Logan, UT, United States), penicillin-streptomycin solution (Gibco, CA, United States), and 2.5% horse serum (Gibco, Carlsbad, CA, United States) was included for MIA $PaCa_2$. All cell lines were cultured at 37 °C under 5% CO_2. The cells were routinely tested using MycAway (Yeasen, Shanghai, China) to eliminate mycoplasma contamination. Paired tumor and adjacent normal tissue samples were collected from the Shanghai General Hospital, and informed consent was obtained from the patients. The study was approved by the Ethics Committee of Shanghai General Hospital of Shanghai Jiao Tong University.

Cell viability assay

The cells were seeded into 96-well plates at a density of 3×10^3 cells/well and incubated overnight. Varying doses of L48H37 (Sigma Aldrich, St Louis, MO, United States) reconstituted in DMSO (Yeasen, Shanghai, China) were added, along with 0.1% DMSO as the negative control, and the cells were cultured for another 24, 48 or 72 h. CCK-8 reagent (Dojindo, Tokyo, Japan) was then added, and the absorbance at 450 nm was measured after 2 h incubation. The IC_{50} values were calculated with the help of a sigmoidal dose-response variable slope model using GraphPad PRISM6 (GraphPad Software, La Jolla, CA, United States)[31].

Colony formation assay

SW1990 and Aspc-1 cells were seeded into 6-well plates at a density of 5×10^2 cells/well in RPMI1640, and incubated overnight. Following a 24 h L48H37 treatment, the medium was replaced with fresh medium, and the cells were cultured for 1 wk. The plates were fixed with 4% paraformaldehyde (Sangon Biotech, Shanghai, China), and the colonies were stained with crystal violet (Sangon Biotech, Shanghai, China) and then counted[30].

Annexin V/7-AAD and propidium iodide staining

Annexin V-PE and 7-AAD (BD PharMingen, San Diego, CA, United States) double staining was performed to detect apoptotic cells, and propidium iodide (PI) (BD PharMingen, San Diego, CA, United States) was used for cell cycle profile analysis, each according to the manufacturer's instructions. The stained cells were analyzed using a BD Accuri C6 Flow Cytometer, and both the percentage of apoptotic cells and the cell cycle profile were analyzed using FlowJo software (Treestar Inc., Ashland, OR, United States)[32].

Western blotting

Cells were lysed with RIPA buffer (Beyotime, Shanghai, China), and protein lysates were resolved by 6%-15% SDS-PAGE and transferred to PVDF membranes (Merk Millipore, Billerica, MA, United States). The latter were blocked and incubated overnight at 4 °C with primary antibodies against the following: β-actin (HRP-60008), Histone H3 (17168-1-AP), PERK (20582-1-AP), EIF2A (11233-1-AP), ATF4 (10835-1-AP), CHOP (15204-1-AP), Caspase8 (66093-1-Ig), Caspase9 (66169-1-Ig), KMT2D (27266-1-AP; all from Proteintech Group, Wuhan, China), BAX (AF1270), Bcl-2 (AF0060; both from Beyotime Inc., Shanghai, China), cleaved caspase-3 (#9661; Cell Signaling Technology, Danvers, MA, United States), p-PERK-ser713 (Biolegend, San Diego, CA, United States), p-EIF2A-ser51 (NOVUS biological Inc., Littleton, CO, United States), and H3K4me1-A2355 (ABclonal, Cambridge, MA, United States)[15]. The immuno-positive bands were detected by incubating with HRP-conjugated secondary antibody (Yeasen, Shanghai, China) for 2 h, followed by color development using ECL reagent (Merk Millipore, Billerica, MA, United States). Protein expression levels were calculated relative to that of β-actin and histone H3.

Mitochondrial membrane potential analysis

The mitochondrial membrane potential (MMP) was analyzed using the JC-1 (BD PharMingen, San Diego, CA, United States) probe, as previously described. The treated cells were harvested and stained with JC-1 for 15 min, and evaluated by flow cytometry and fluorescence microscopy (200 × magnification)[30].

Measurement of reactive oxygen species generation

Intracellular reactive oxygen species (ROS) levels were assayed using the DCFH-DA fluorescent probe (Sigma Aldrich, St Louis, MO, United States), as previously described. The treated L48H37, SW1990 and Aspc-1 cells were incubated with the dye for 30 min, and then analyzed with the BD Accuri C6 Flow Cytometer, followed by analysis with FlowJo software[30].

Small interfering RNA transfection

SW1990 and Aspc-1 cells were seeded into 6-well plates, and transfected with si-ATF4 or control small interfering RNA (siRNA) using lipofectamine 2000 (Invitrogen, Carlsbad, CA, United States) once the cells reached 70%-90% confluency. Briefly, 100 pmol siRNA was mixed with 5 μL lipofectamine 2000, and the cells were incubated with the mixture for 48 h[15]. The siRNA duplexes (GenePharma, Shanghai, China) had the following sequences: Control siRNA: 5′-UUCUCCGAACGUGUCACGUTT-3′ (sense); 5′-ACGUGACACGUUCGGAGAATT-3′ (anti-sense); ATF4 siRNA # 15′-CUGCUUACGUUGCCAUGAUTT-3′ (sense) 5′-AUCAUGGCAACGUAAGCAGTT-3′ (anti-sense); ATF4 siRNA # 25′-CUCCCAGAAAGUUUAACAATT-3′ (sense) 5′-UUGUUAAACUUUCUGGGAGTT-3′ (anti-sense).

Real-time quantitative PCR analysis

Total RNA was extracted from PDAC cell lines using the RNAiso Plus Reagent (Takara Bio Inc., Shiga, Japan) according to the manufacturer's instructions, and 500 ng RNA per sample was reverse-transcribed into cDNA using the PrimeScript™ RT Reagent Kit (Takara Bio Inc., Shiga, Japan). The cDNA samples were amplified using SYBR® Premix Ex Taq™ II (Takara Bio Inc., Shiga, Japan), and relative mRNA expression was determined by the $2^{-\Delta\Delta Ct}$ method using β-actin as the internal control[33].

Immunofluorescence

Cells were grown on glass slides and fixed with 4% paraformaldehyde for 15 min, followed by permeabilization with 0.5% Triton X-100 (Sangon Biotech, Shanghai, China) for 20 min at room temperature. The cells were blocked and then incubated overnight with the specific primary antibody at 4 °C, followed by another incubation with the secondary antibody and counterstaining with DAPI (Sangon Biotech, Shanghai, China). The stained cells were observed under a fluorescence microscope[34].

Lentiviral transduction

Cells grown to 30%-50% confluency were transduced with the appropriate amount of pLKD-CMV-EGFP-U6-shKMT2D or pLKD-CMV-EGFP-U6-shCTRL lentivirus (Obio Technology, Shanghai, China) with 6 μg/mL polybrene (Hanbio, Shanghai, China). The stably transfected cells were selected by 5 μg/mL puromycin (Sigma Aldrich, St Louis, MO, United States) for at least 2 wk[35].

Bioinformatics analysis

The RNA sequencing (RNA-Seq) data on the metastatic PDAC Colo357 and SUIT-2 cell lines were downloaded from the GEO database[36], and the differentially expressed

genes (DEGs) were screened using Morpheus software[37]. Overlapping DEGs were depicted by online Venn diagram analysis[38], and gene enrichment analysis was performed online using Metascape[39]. Differential levels of KMT2D between tumor and normal tissues were obtained from the GEPIA[40] and Oncomine databases[41], and the KMT2D expression levels and clinical characteristics of PDAC patients were obtained from the TCGA database[42]. The prognostic value of KMT2D was determined using Kaplan Meier survival analysis.

Wound healing assay

Cell migration was determined using scratch assays, as previously described. Control or KMT2D-knockdown SW1990 cells were cultured in 6-well plates until 70% confluency, and treated with L48H37 or DMSO for 24 h. Once the cells were nearly 90% confluent, the monolayer was scratched using a sterile pipette tip. The number of cells migrating into the "wound" area were counted for 2 consecutive days by manual tracking using Fiji software (National Institutes of Health, Bethesda, MD, United States)[43].

Tumor inhibition assay in vivo

Five-week-old BALB/c nude mice were provided by the Institutional Animal Care and Use Committee of Shanghai General Hospital, housed at constant temperature with a 12 h light/dark cycle, and given standard rodent diet and water ad libitum. The mice were randomized into the L48H37-treated (n = 5) and negative control (n = 5) groups, and every animal was injected with cells transduced with ctrl-shRNA and KMT2D-shRNA lentiviruses on opposite flanks. When tumors in the negative control group reached a volume of 50-100 mm^3, five mice were injected with 5 mg/kg L48H37 intraperitoneally on alternate days, and five with the same volume of physiological saline: the final groups were shCTRL, shKMT2D, shCTRL + L48H37 and shKMT2D + L48H37. The tumor volume V was calculated as $0.5 \times l \times w^2$, where l and w are the length and width at the indicated time points, respectively. At the end of treatment, the animals were sacrificed under anesthesia, and tumors were removed and weighed. All animal experiments complied with the Shanghai Jiao Tong University's Policy on the Care and Use of Laboratory Animals[30].

Immunohistochemistry

PDAC and matched normal pancreatic tissue sections were deparaffinized and rehydrated, bleached with 3% H_2O_2 to remove endogenous catalase activity, and boiled in citrate buffer for antigen retrieval. After blocking with serum for 30 min, tissue sections were incubated overnight with primary antibodies against KMT2D and H3K4me1 at 4 °C. Sections were washed with PBS and incubated with HRP-conjugated secondary antibody for 50 min, followed by color development using DAB. The immuno-stained sections were observed under an optical microscope (200 × and 400 × magnification) and analyzed by Fiji software[18].

Statistical analysis

Statistical analyses were performed using the IBM SPSS Statistics v23 software (IBM Corp., Armonk, NY, United States), program R and GraphPad PRISM 6. The continuous variables were expressed as mean ± SEM of at least three biological replicates, and compared using the Student's t-test and one-way ANOVA. Categorical variables were analyzed using the Chi-square test or Fisher's exact test. Survival curves were plotted using the Kaplan-Meier method, and evaluated by the log-rank test. P values of less than 0.05 were considered statistically significant.

RESULTS

L48H37 inhibits proliferation and promotes apoptosis in PDAC cells in vitro

L48H37 is a novel curcumin analogue with greater stability, and has shown potent anti-tumor activity against lung cancer[30]. The molecular structures of curcumin and L48H37 are shown in Supplement Figure 1A and 1B. The IC_{50} of L48H37 in the metastatic SW1990 and Aspc-1 cell lines ranged from 12.2-16.34 μm and 3.8-9.45 μm, respectively, after 3 consecutive days of treatment. In the primary PANC-1 and MIA $PaCa_2$ cell lines, the IC_{50} values ranged from 7.89-976.5 μm and 9.17-333.7 μm, respectively (Figure 1A-D). Thus, L48H37 acted more rapidly in the metastatic cells compared to the primary PDAC cells, indicating a tumor stage-specific mode of action. Furthermore, L48H37 also inhibited the colony forming abilities of the SW1990 and Aspc-1 cells in a dose-dependent manner (Figure 1E). Annexin V/7-AAD staining showed that L48H37 increased apoptosis in PDAC cells in a dose-dependent manner (Figure 1F and G), which corresponded with a significant increase in the levels of Bax

and cleaved caspase 3, and a decrease in Bcl-2 and Bcl-2/Bax ratio in treated PDAC cells (Figure 1H and I).

L48H37 alters MMP, increases ROS production, induces cell cycle arrest and activates the ER stress pathway in PDAC cells

To further elucidate the specific mechanism of L48H37 action, we analyzed the MMP changes (ψm), ROS levels, cell cycle profile and ER stress pathway in treated PDAC cells. As shown in Figures 2A and B, L48H37 significantly disrupted mitochondrial homeostasis and increased MMP loss, eventually leading to apoptosis. ROS accumulation in tumor cells mediates oxidative damage and MMP loss, which is one of the underlying mechanisms of anti-cancer drugs[44]. As shown in Figure 2C-E, L48H37 treatment increased intracellular ROS levels over 30% from the baseline in a dose-dependent manner, indicating that L48H37 increases oxidative stress and induces apoptosis in PDAC cells by activating the mitochondrial apoptotic pathway. In addition, L48H37 also upregulated caspase 9 and caspase 8 in a dose-dependent manner, which may contribute to a cross-talk between the intrinsic and extrinsic apoptotic pathways (Figure 2K). Cell cycle arrest is another mechanism used by anti-neoplastic agents to control cancer cell proliferation. We found that L48H37 induced a G2 /M arrest in two PDAC cell lines (Figure 2F, G and H), indicating that it also inhibits cancer cell proliferation by inducing cell cycle arrest.

ER stress is a critical factor leading to apoptosis. The activation of PERK phosphorylates the eukaryotic initiation factor 2α (EIF2A), and inhibits protein translation to promote cell survival. However, EIF2A can also induce activating transcription factor-4 (ATF-4) and enhancer-binding protein-homologous protein (CHOP) expression, which increase protein synthesis and lead to cell death[45,46]. As shown in Figure 2I and J, L48H37 significantly upregulated p-PERK, p-EIF2A, ATF4 and CHOP in SW1990 cells in a time- and dose-dependent manner, indicating a role of the ER stress pathway in mediating the effects of L48H37.

ATF-4 knockdown attenuates L48H37-induced apoptosis and upregulates KMT2D

To validate a potential role of the ER stress pathway in L48H37-induced apoptosis in pancreatic cancer cells, we silenced ATF4 in SW1990 and ASPC-1 cells (Supplement Figure 2A and B). Interestingly, ATF4 knockdown significantly upregulated KMT2D (Figure 3A-C), and decreased apoptosis in human pancreatic cancer cells (Figure 3D). KMT2D is associated with low proliferation rates and sensitivity of pancreatic cancer cells to the antimetabolite 5-fluorouracil (5-FU)[15,47]. However, little is known regarding the relationship between histone methyltransferases and the ER stress pathway[48-51]. We also analyzed the expression levels of the PERK/eIF2a/ATF4/CHOP signaling pathway mediators in ATF4 knockdown cells following L48H37 treatment, and found that the proteins upstream of ATF4 were unaltered, whereas those downstream were significantly decreased (Figure 3E-F). This indicated that ATF4 knockdown unidirectionally downregulated the ER stress pathway, and that KMT2D was downstream of ATF4. Based on these findings, we hypothesized that L48H37 induces apoptosis *via* the ER stress pathway, and depletion of KMT2D sensitizes the cells to L48H37.

KMT2D knockdown enhances L48H37-induced apoptosis in pancreatic cancer cells

To further investigate the role of KMT2D in L48H37-induced apoptosis, we first analyzed the basal expression of KMT2D in different PDAC lines. KMT2D levels were higher in the metastatic cell lines compared to the primary cell lines (Supplement Figure 3A). L48H37 treatment slightly decreased KMT2D expression along with that of H3K4me1 (Figure 4A-C). In addition, knocking down KMT2D in the SW1990 and ASPC-1 cells lines (Supplement Figure 3B and C) significantly decreased their viability for 3 consecutive days (Figure 4D and 4E), and augmented L48H37-induced apoptosis (Figure 4F). These findings indicated a synergistic relationship between KMT2D knockdown and L48H37. Consistent with this, KMT2D knockdown also upregulated p-PERK, p-EIF2A, ATF4 and CHOP (Figure 4G and H), and triggered cell cycle arrest at the G0/G1 or G2/M phases in L48H37-treated cells (Figure 4I and J). Taken together, KMT2D deficiency is essential for L48H37-induced apoptosis, cell cycle arrest and activation of the ER stress pathway. A smaller pool of cells in the S and mitotic phases following KMT2D knockdown eventually sensitized the cells to L48H37-induced apoptosis.

KMT2D knockdown synergizes with L48H37 to promote apoptosis and inhibit migration

To further explore the effects of KMT2D deficiency in pancreatic cancer, we downloaded RNA-Seq data on KMT2D-silenced and normal Colo357 and SUIT-2 metastatic PDAC cell lines from the GEO database GSE75327, and screened for DEGs.

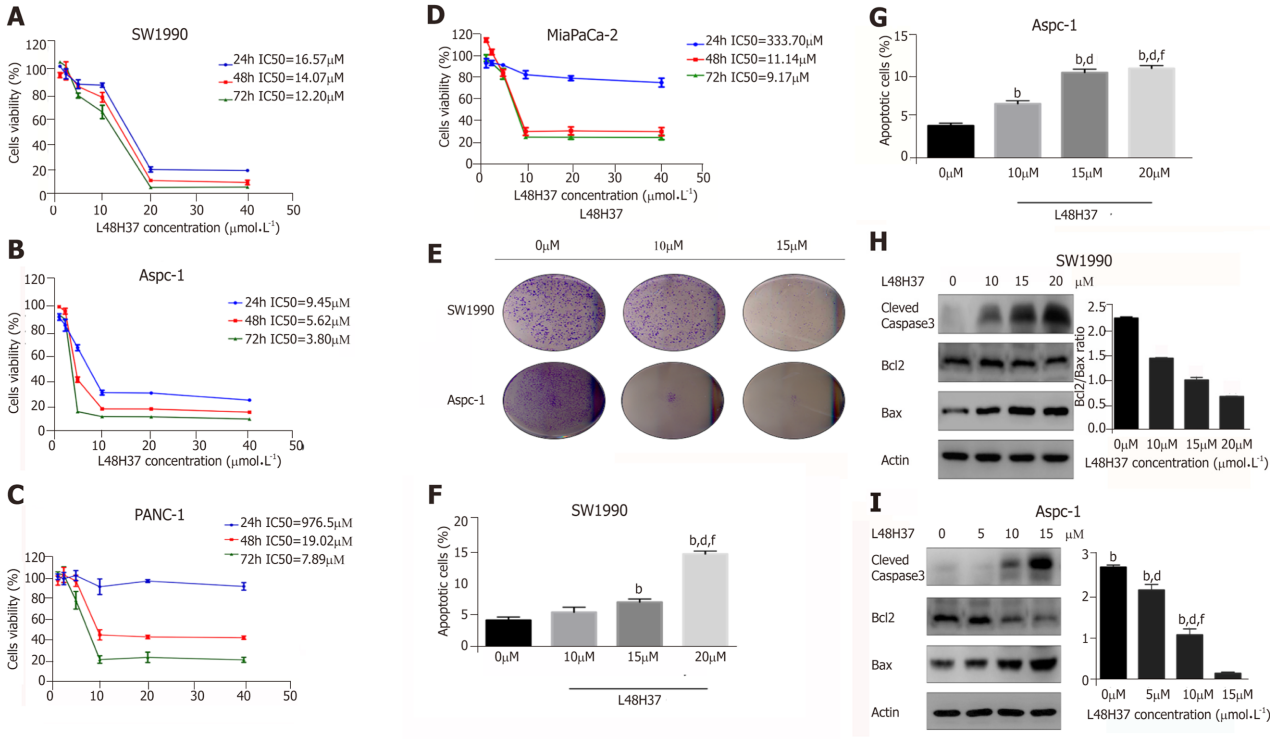

Figure 1 L48H37 inhibits proliferation and promotes apoptosis in pancreatic cancer cells. A-D: Percentage of viable SW1990, ASPC-1, PANC-1 and MIA $PaCa_2$ cells incubated with different concentrations of L48H37 (1.25, 2.5, 5, 10, 20 and 40 μmol/L) or DMSO (negative control) for 24, 48 and 72 h. The IC_{50} values in the different cell lines are shown; E: Representative pictures of colonies from SW1990 and ASPC-1 cells treated with increasing concentrations of L48H37 for 24 h; F-G: SW1990 and Aspc-1 cells were treated with various concentrations of L48H37 for 24 h. Cell apoptosis was detected by flow cytometry. Histogram illustrating the rate of apoptosis cells. Data were expressed as mean ± SEM; F: $^{b}P < 0.01$ *vs* L48H37 (0 μmol/L) group. $^{d}P < 0.01$ *vs* L48H37 (10 μmol/L) group. $^{f}P < 0.01$ *vs* L48H37 (15 μmol/L) group; G: $^{b}P < 0.01$ *vs* L48H37 (0 μmol/L) group; $^{d}P < 0.01$ *vs* L48H37 (5 μmol/L) group. $^{f}P < 0.01$ *vs* L48H37 (10 μmol/L) group; H-I: Western blotting showing expression levels of Cleaved caspase3, Bcl-2 and Bax proteins in SW1990 and Aspc-1 cells following treatment with DMSO or L48H37 for 12 h. Grayscale values of Bcl-2 and Bax were measured relative to β-actin, and the ratio of Bcl-2/Bax expression was calculated. Data were expressed as mean ± SEM; H: $^{b}P < 0.01$ *vs* L48H37 (0 μmol/L) group. $^{d}P < 0.01$ *vs* L48H37 (10 μmol/L) group. $^{f}P < 0.01$ *vs* L48H37 (15 μmol/L) group; I: $^{b}P < 0.01$ *vs* L48H37 (0 μmol/L) group. $^{d}P < 0.01$ *vs* L48H37 (5 μmol/L) group. $^{f}P < 0.01$ *vs* L48H37 (10 μmol/L) group.

The heat map of the top 200 DEGs is shown in Supplement Figure 4A. A total of 579 genes were upregulated (blue), and 273 genes were downregulated (yellow) in Colo357 cells (Figure 5A), while 680 and 292 genes were upregulated (red) and downregulated (green) in SUIT-2 cells, respectively (Figure 5B). The functional classification of the upregulated genes showed an enrichment in the extrinsic apoptotic signaling pathway in the absence of ligand, and included PPP2R1B, IL1A, MAPK8IP2, MCL1, ELL3, PDCD6, HIC1 and PTPMT1. The downregulated genes, including TULP1, AQP2 and ALOX12B, were mainly involved in multicellular organismal homeostasis (Figure 5C and D). To determine the role of KMT2D in tumor metastasis, wound healing assays were carried out with control and KMT2D knockdown PDAC cells. *In vitro* migration was significantly decreased after KMT2D silencing, which also increased the anti-migratory effects of L48H37 (Figure 5E-F).

KMT2D knockdown synergizes with L48H37 to inhibit PDAC xenograft growth in vivo

Male BALB/c nude mice were injected with control and KMT2D knockdown PDAC cells, followed by L48H37 or placebo injections. Both tumor weight and volume were significantly decreased in the shKMT2D group compared to the shCTRL group ($P < 0.01$). L48H37 treatment further decreased the tumor load, especially in the shKMT2D group ($P < 0.05$) (Figure 6A-C). Therefore, KMT2D depletion inhibited tumor growth synergistically with L48H37. In addition, no systemic adverse effects were observed in mice, consistent with a previous study that reported no structural damage to essential organs in mice treated with L48H37[30].

KMT2D expression is not related to clinico-pathological features and patient prognosis

Studies have reported high mutation rates of KMT2D in PDAC, and KMT2D expression levels correlate with tumor initiation and progression[3]. Data from the

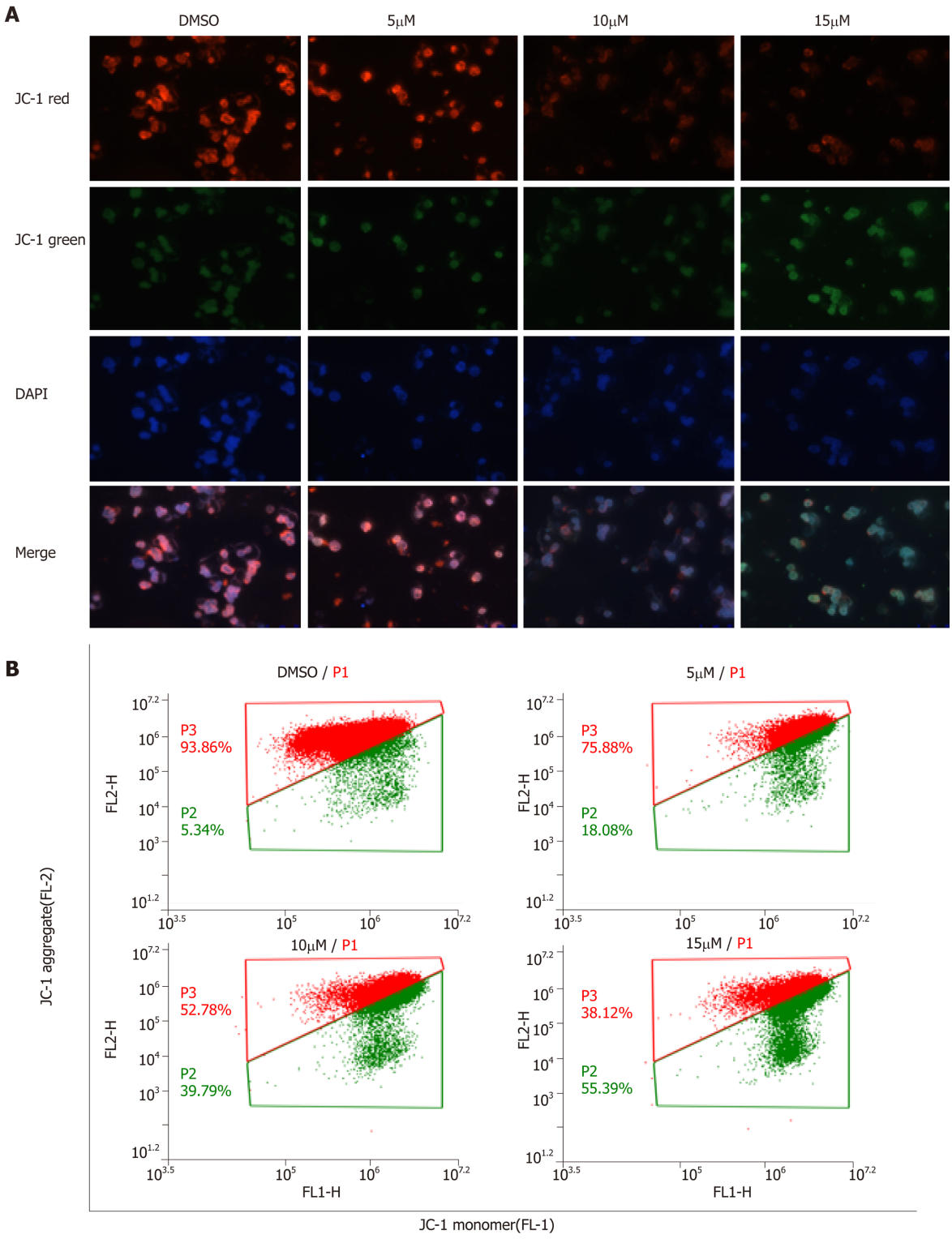
A
DMSO
5μM
10μM
15μM
JC-1 red
JC-1 green
DAPI
Merge
B
DMSO / P1
5μM / P1
10μM / P1
15μM / P1
P3
93.86%
P2
5.34%
P3
75.88%
P2
18.08%
P3
52.78%
P2
39.79%
P3
38.12%
P2
55.39%
FL2-H
FL1-H
JC-1 aggregate(FL-2)
JC-1 monomer(FL-1)
C
4.0k
3.0k
2.0k
1.0k
0
DMSO
L48H37-10μM
L48H37-15μM
L48H37-20μM

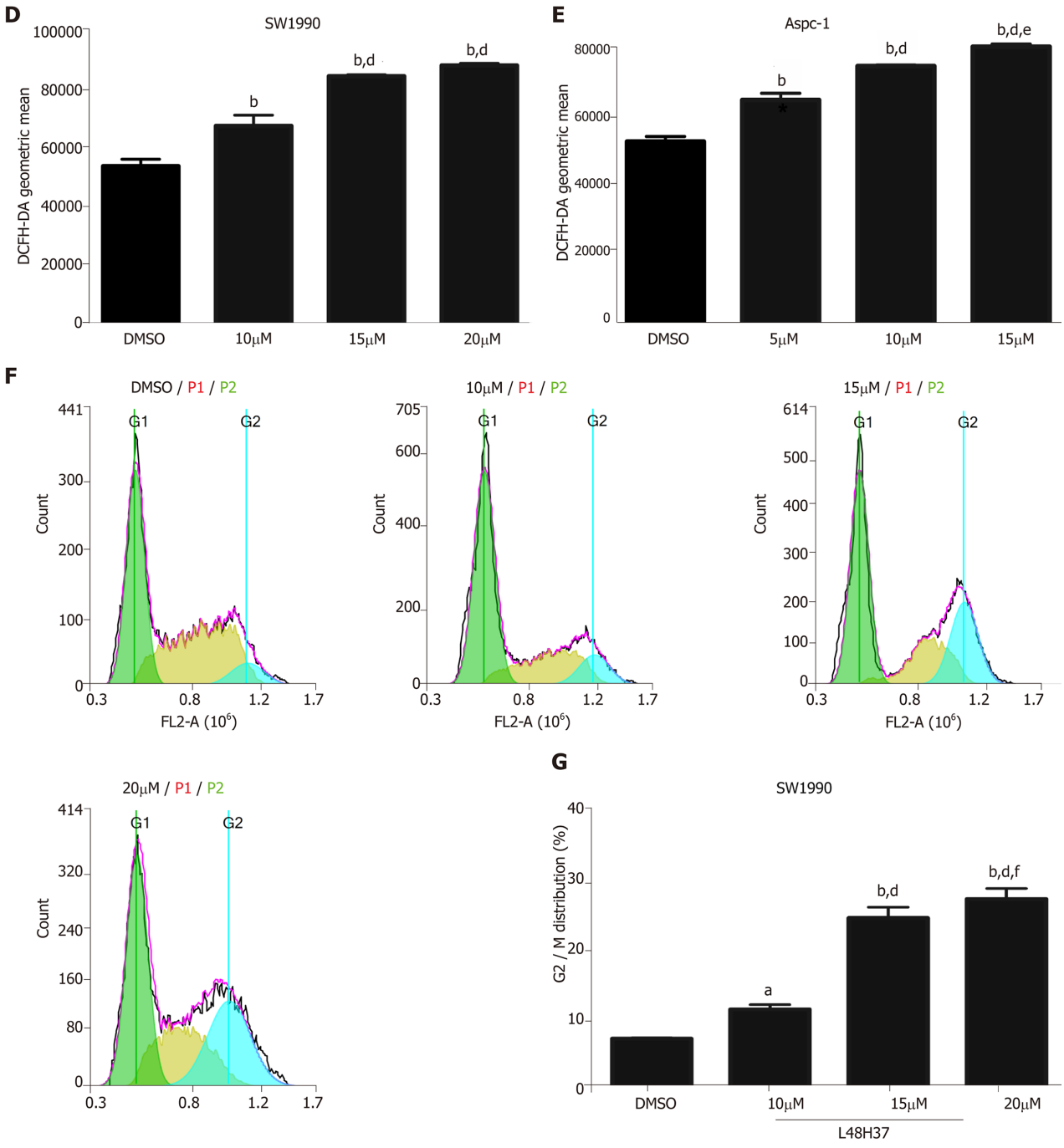
D
SW1990
DCFH-DA geometric mean
100000
80000
60000
40000
20000
0
b
b,d
b,d
DMSO
10μM
15μM
20μM
E
Aspc-1
DCFH-DA geometric mean
80000
60000
40000
20000
0
b
b,d
b,d,e
DMSO
5μM
10μM
15μM
F
DMSO / P1 / P2
10μM / P1 / P2
15μM / P1 / P2
20μM / P1 / P2
Count
G1
G2
FL2-A (10^6)
G
SW1990
G2 / M distribution (%)
40
30
20
10
0
a
b,d
b,d,f
DMSO
10μM
15μM
20μM
L48H37

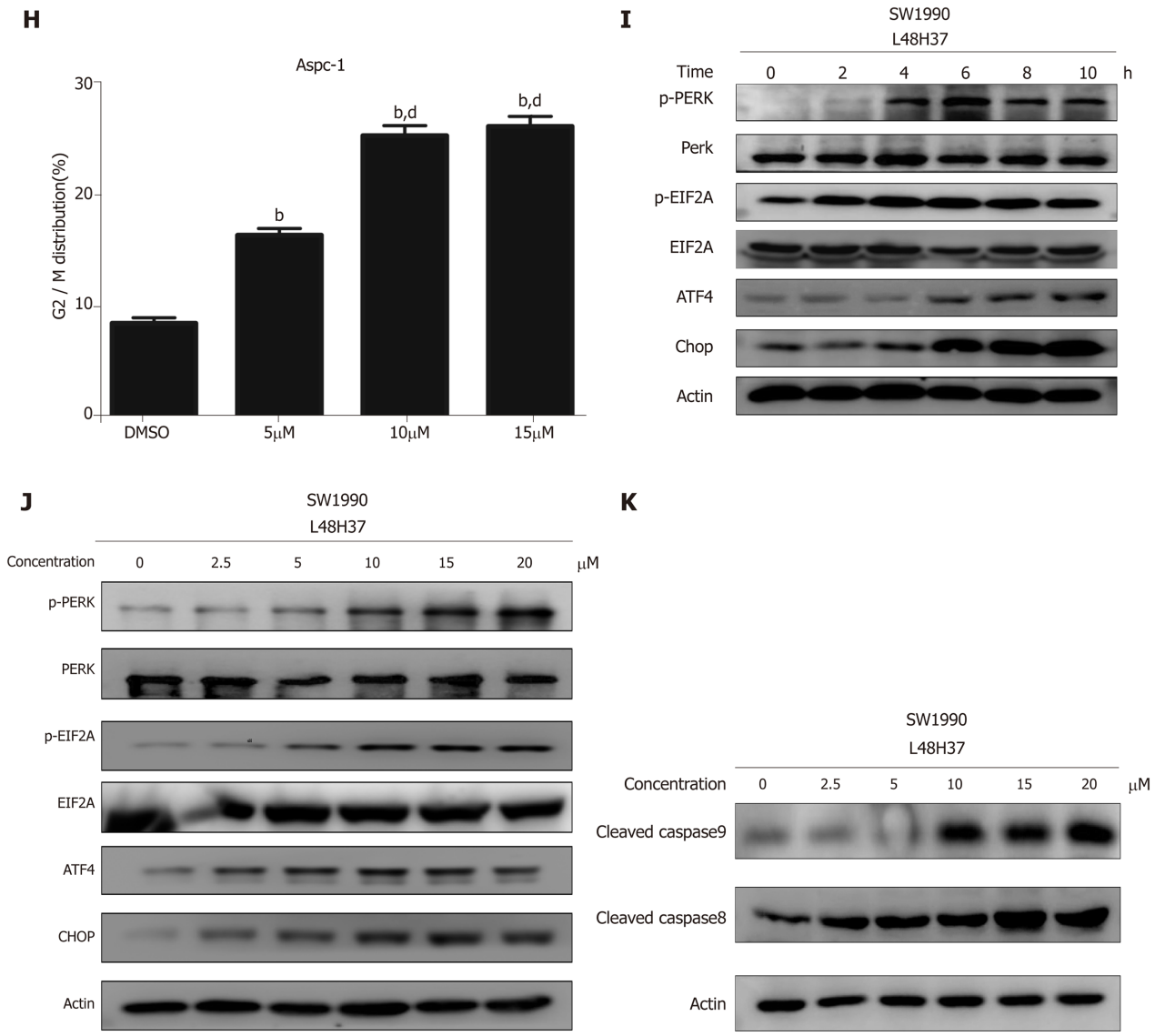

Figure 2 L48H37 alters mitochondrial membrane potential, reactive oxygen species levels, cell cycle profile arrest and endoplasmic reticulum stress pathway in pancreatic ductal adenocarcinoma cells. A, B: Representative images and FACS plots of SW1990 cells treated with 5, 10 and 15 μmol/L L48H37 and stained with JC-1 probe (200× magnification); C, E: Reactive oxygen species (ROS) generation induced by L48H37 within 12 h was measured in SW1990 and Aspc-1 cells by staining with DCFH-DA (25 μmol/L) for 30 min. ROS level was acquired by flow cytometry. Histogram showing the DCFH-DA geometric mean in cells treated with different L48H37 concentrations. Data were expressed as mean ± SEM; D: $^{b}P < 0.01$ *vs* DMSO group. $^{d}P < 0.01$ *vs* L48H37 (10 μmol/L) group; E: $^{b}P < 0.01$ *vs* DMSO group. $^{d}P < 0.01$ *vs* L48H37 (5 μM) group. $^{e}P < 0.05$ *vs* L48H37 (10 μmol/L) group; F-H: SW1990 and Aspc-1 cells were harvested 24 h with L48H37 or DMSO, and then cycle distribution was assessed by Propidium Iodide staining. Histogram illustrating the rate of G2/M phase cells. Data were expressed as mean ± SEM; G: $^{b}P < 0.01$ *vs* DMSO group. $^{d}P < 0.01$ *vs* L48H37 (10 μmol/L) group. $^{f}P < 0.01$ *vs* L48H37 (15 μmol/L) group; H: $^{b}P < 0.01$ *vs* DMSO group. $^{d}P < 0.01$ *vs* L48H37 (5 μmol/L) group; I-K: SW1990 cells were treated with L48H37 for the indicated times or treated with various concentrations of L48H37 or DMSO. The protein levels of p-PERK, PERK, p-EIF2α, EIF2α, ATF4, CHOP, cleaved caspase-9, and cleaved caspase-8 were analyzed by Western blot. β-actin was used as an internal control.

ICGC database showed that lower KMT2D levels correlated to better overall survival in pancreatic cancer patients[15]. Based on our *in vitro* findings, we hypothesized that KMT2D deficiency sensitizes tumor cells to chemotherapeutic drugs or other treatments, and improves prognosis. To this end, we analyzed KMT2D expression levels in a PDAC patient cohort, and found significantly elevated levels in tumor tissues compared to adjacent normal tissues ($P < 0.01$). Accordingly, H3K4me1 levels were also markedly elevated in tumor tissues ($P < 0.01$) (Figure 7A-D). Similar results were obtained from PDAC patient data downloaded from the TCGA and Oncomine databases (Figure 7E and F).

To determine the clinical significance of KMT2D in PDAC, we analyzed the RNA-Seq data of 106 patients from the TCGA database, and classified them into KMT2D^{high} and KMT2D^{low} groups using the median KMT2D mRNA expression level. We found no correlation between KMT2D levels and overall or disease-free survival (Figure 7G

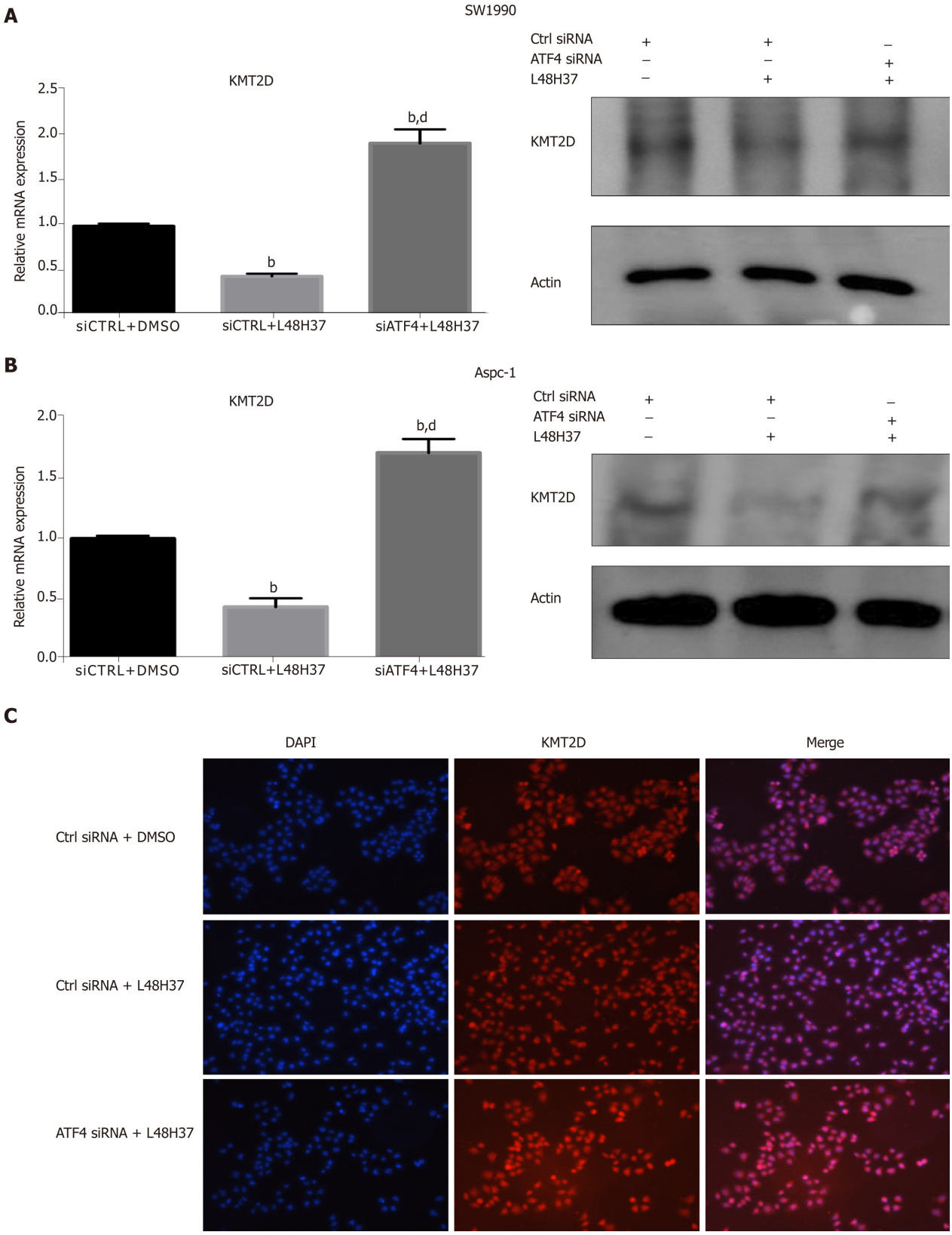
A
SW1990
KMT2D
Relative mRNA expression
2.5
2.0
1.5
1.0
0.5
0.0
b,d
b
siCTRL+DMSO
siCTRL+L48H37
siATF4+L48H37
Ctrl siRNA + + –
ATF4 siRNA – – +
L48H37 – + +
KMT2D
Actin
B
Aspc-1
KMT2D
Relative mRNA expression
2.0
1.5
1.0
0.5
0.0
b,d
b
siCTRL+DMSO
siCTRL+L48H37
siATF4+L48H37
Ctrl siRNA + + –
ATF4 siRNA – – +
L48H37 – + +
KMT2D
Actin
C
DAPI
KMT2D
Merge
Ctrl siRNA + DMSO
Ctrl siRNA + L48H37
ATF4 siRNA + L48H37

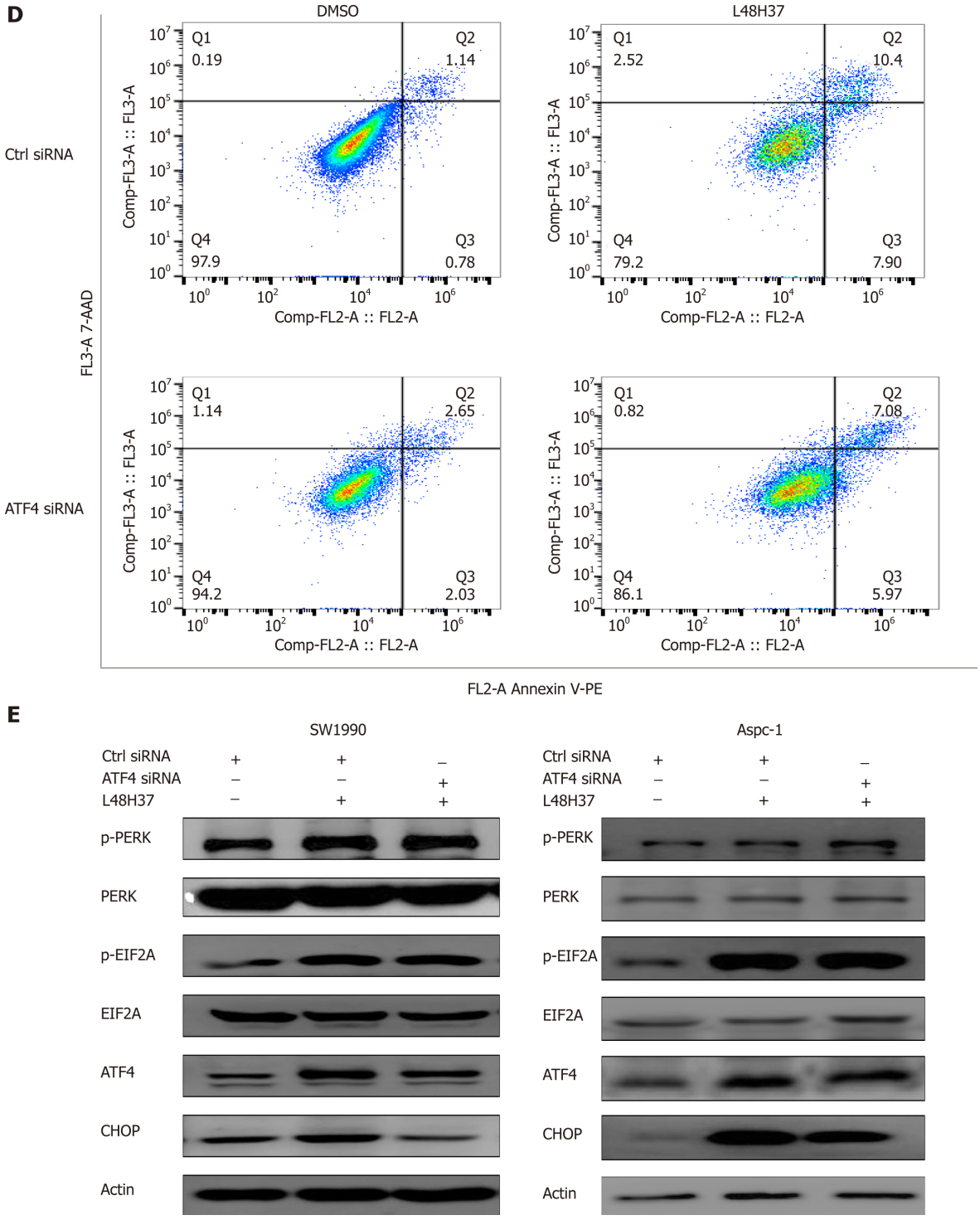

Figure 3 ATF-4 knockdown attenuates L48H37-induced apoptosis and upregulates KMT2D. A, B: KMT2D mRNA and protein levels in the control and ATF-4-knockdown SW1990 and ASPC-1 cells treated with 15 μM L48H37 for 12 h. β-actin was used as an internal control. Data were expressed as mean ± SEM. $^{b}P < 0.01$ *vs* siCTRL + DMSO group. $^{d}P < 0.01$ *vs* siCTRL + L48H37 group; C: Representative IF image showing KMT2D expression in control and ATF4-knockdown SW1990 cells treated with L48H37; D: FACS plot showing apoptosis in control and ATF4 knockdown SW1990 cells treated with L48H37; E, F: Western blotting showing levels of p-PERK, PERK, p-EIF2α, EIF2α, ATF4 and CHOP in control and ATF4 knockdown SW1990 cells treated with L48H37. β-actin was used as an internal control. PERK: Protein kinase RNA-like endoplasmic reticulum kinase; EIF2A: Eukaryotic initiation factor 2α; ATF-4: Activating transcription factor-4; CHOP: Enhancer-binding protein-homologous protein.

and H). In addition, higher KMT2D expression was found to be associated with poor tumor grading in clinico-pathological features analysis (Supplement Table 1).

DISCUSSION

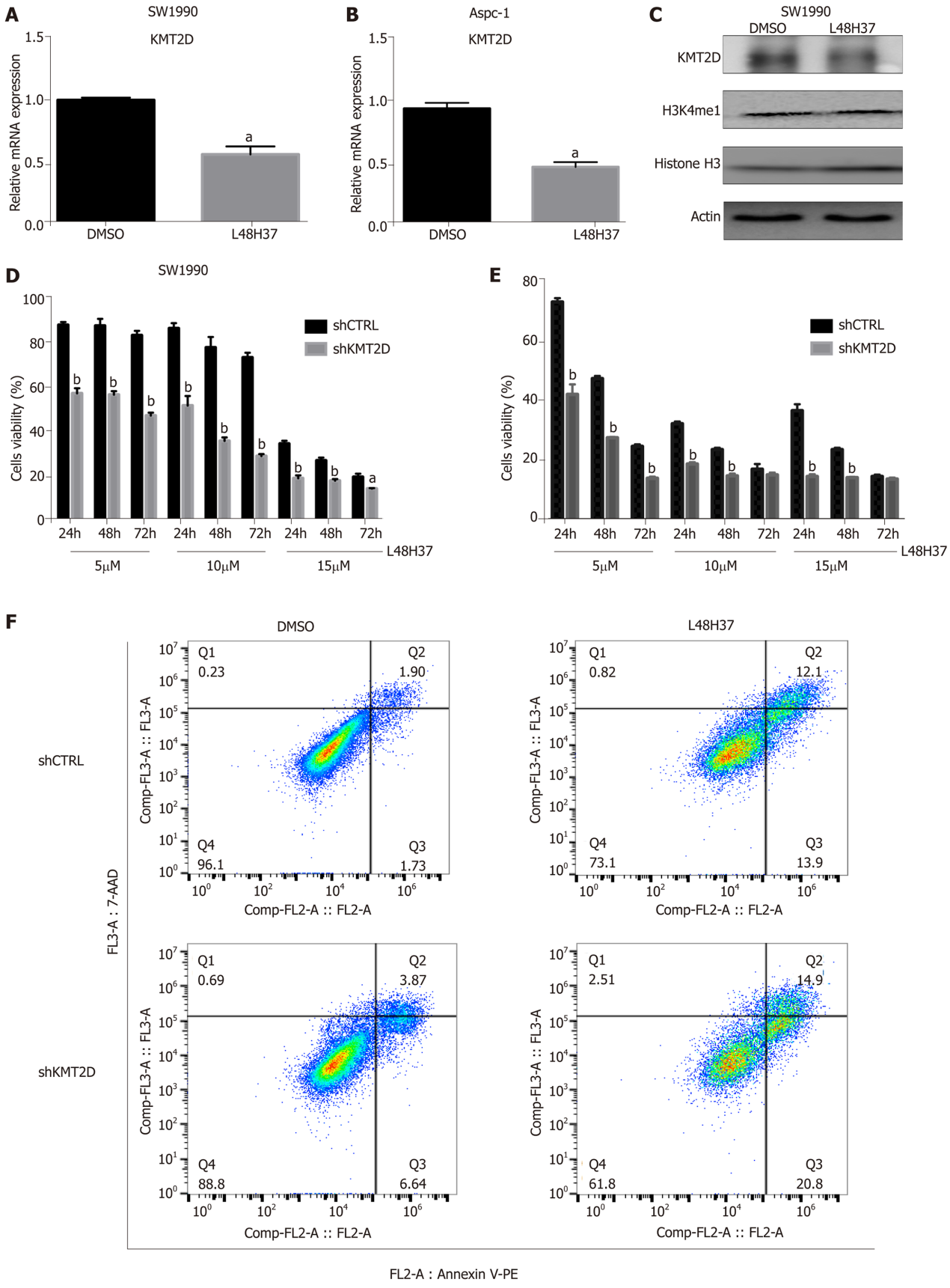
A
SW1990
KMT2D
Relative mRNA expression
DMSO
L48H37
B
Aspc-1
KMT2D
C
SW1990
DMSO
L48H37
KMT2D
H3K4me1
Histone H3
Actin
D
SW1990
shCTRL
shKMT2D
Cells viability (%)
24h
48h
72h
5μM
10μM
15μM
L48H37
E
F
DMSO
L48H37
shCTRL
shKMT2D
FL3-A : 7-AAD
Comp-FL3-A :: FL3-A
Comp-FL2-A :: FL2-A
Q1
Q2
Q3
Q4
0.23
1.90
96.1
1.73
0.82
12.1
73.1
13.9
0.69
3.87
88.8
6.64
2.51
14.9
61.8
20.8
FL2-A : Annexin V-PE

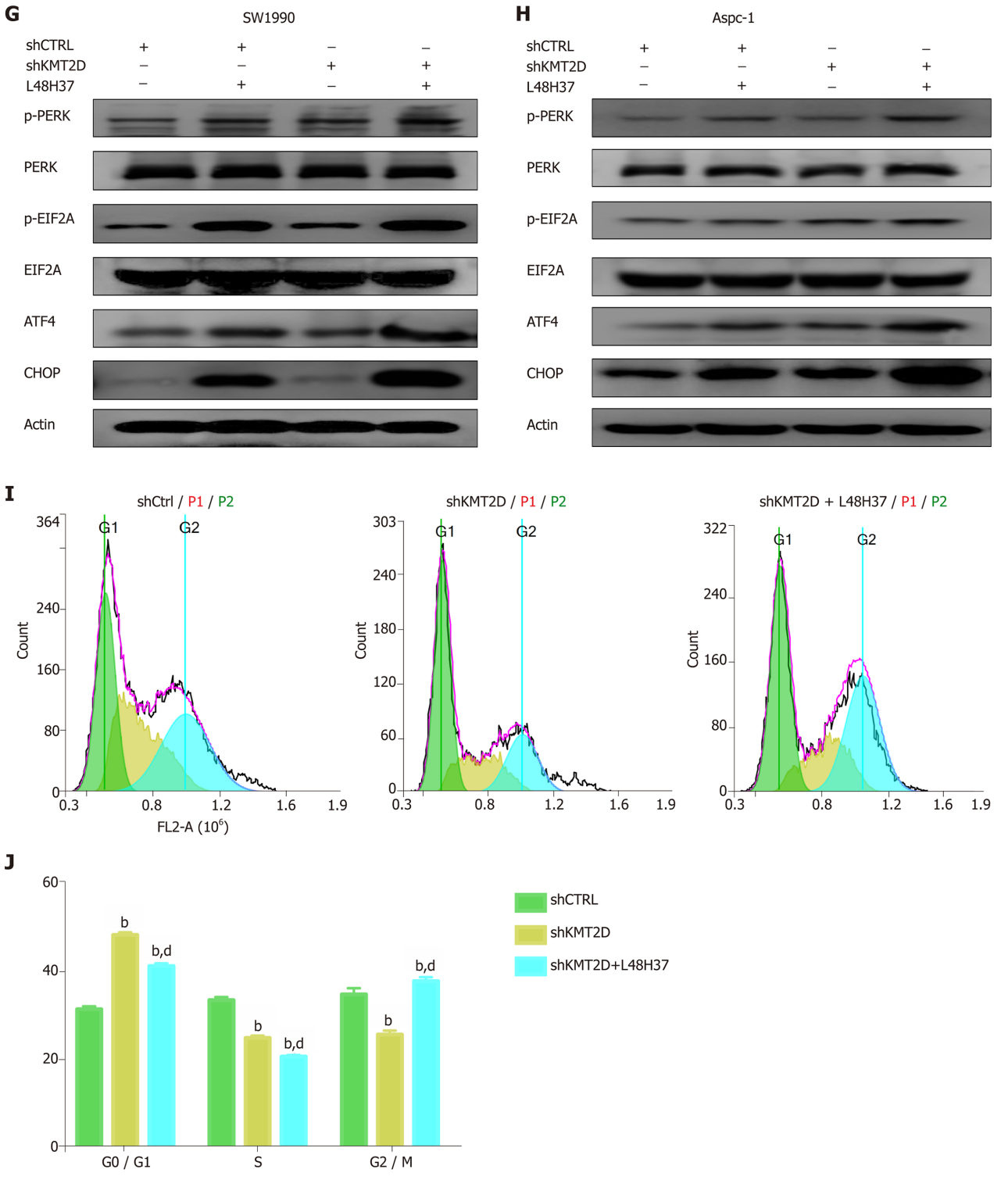

Figure 4 KMT2D knockdown enhances apoptosis in pancreatic ductal adenocarcinoma cells. A-C: Immunoblot showing KMT2D and H3K4me1 protein levels in SW1990 and ASPC-1 cells treated with 15 μM L48H37 for 8 h. β-actin and Histone H3 were used as an internal control. The KMT2D mRNA levels were measured by RT-qPCR 24 h later. Data were expressed as mean ± SEM. [a]*P* < 0.05 *vs* DMSO group; D, E: KMT2D mRNA and protein levels in control and KMT2D-knockdown SW1990 and ASPC-1 cells treated with L48H37 (5, 10 and 15 μmol/L) or DMSO for three consecutive days, and percentage of viable cells. Data were expressed as mean ± SEM. [a]*P* < 0.05 *vs* shCTRL group at the same time point. [b]*P* < 0.01 *vs* shCTRL group at the same time point; F: Apoptosis rates in the control and KMT2D-knockdown SW1990 and ASPC-1 cells; G, H: Western blotting showing levels of p-PERK, PERK, p-EIF2α, EIF2α, ATF4 and CHOP in the control and KMT2D-knockdown SW1990 and ASPC-1 cells. β-actin was used as an internal control; I, J: shKMT2D or shCTRL SW1990 cells were harvested 24 h with L48H37, then cycle distribution was assessed by Propidium Iodide staining. Histogram showing the percentage of control and KMT2D knockdown SW1990 and ASPC-1 cells in the G0/G1, S, and G2/M phases. Data were expressed as mean ± SEM; J: [b]*P* < 0.01 *vs* shCTRL group in the same cell cycle. [d]*P* < 0.01 *vs* shKMT2D group in the same cell cycle. PERK: Protein kinase RNA-like endoplasmic reticulum kinase; EIF2A: Eukaryotic initiation factor 2α; ATF-4: Activating transcription factor-4; CHOP: Enhancer-binding protein-homologous protein.

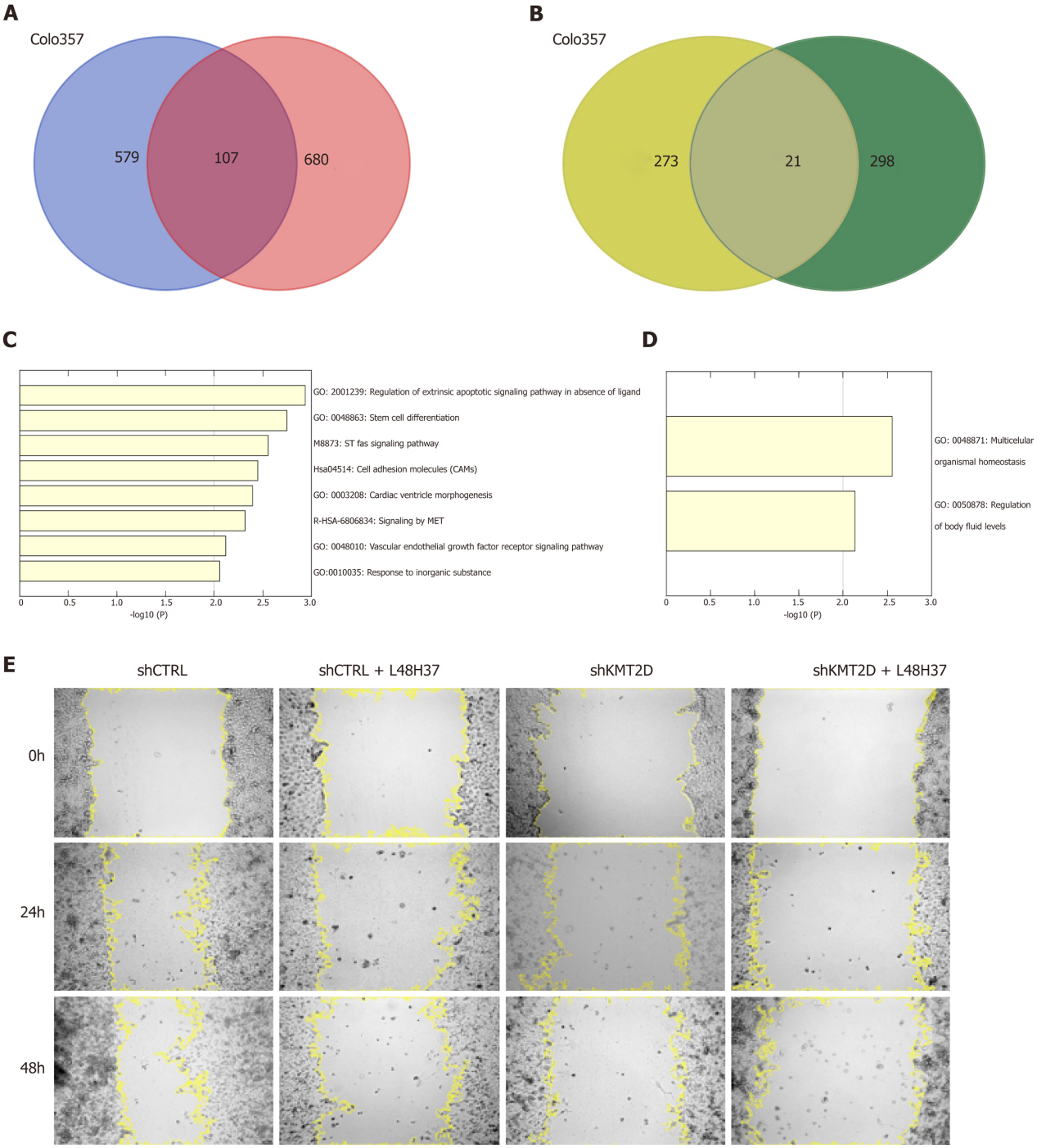
A
Colo357
579
107
680
B
Colo357
273
21
298
C
GO: 2001239: Regulation of extrinsic apoptotic signaling pathway in absence of ligand
GO: 0048863: Stem cell differentiation
M8873: ST fas signaling pathway
Hsa04514: Cell adhesion molecules (CAMs)
GO: 0003208: Cardiac ventricle morphogenesis
R-HSA-6806834: Signaling by MET
GO: 0048010: Vascular endothelial growth factor receptor signaling pathway
GO:0010035: Response to inorganic substance
0
0.5
1.0
1.5
2.0
2.5
3.0
-log10 (P)
D
GO: 0048871: Multicelular organismal homeostasis
GO: 0050878: Regulation of body fluid levels
0
0.5
1.0
1.5
2.0
2.5
3.0
-log10 (P)
E
shCTRL
shCTRL + L48H37
shKMT2D
shKMT2D + L48H37
0h
24h
48h

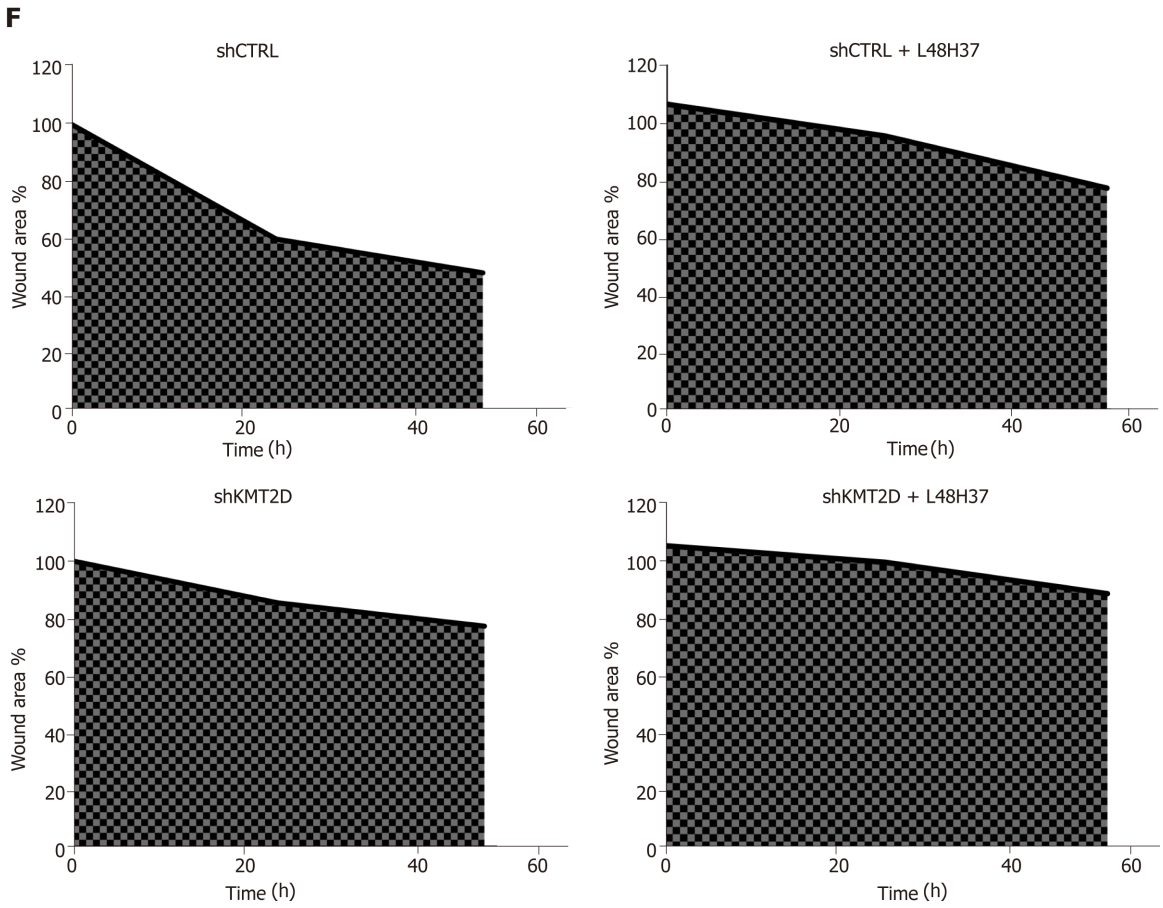

Figure 5 KMT2D knockdown augments L48H37-induced apoptosis and blocks migration *in vitro*. A, B: Venn diagram showing overlapping DEGs in KMT2D knockdown Colo357 and SUIT-2 cells. Upregulated genes are shown in blue and red, and the downregulated in yellow and green in the Colo357 and SUIT-2 cells, respectively; C, D: Functional analysis of the overlapping DEGs; E, F: Graph showing the number of manually tracked migrating control and KMT2D knockdown SW1990 cells treated with L48H37.

Gemcitabine and 5-FU are the standard treatments for advanced pancreatic cancer, but they are ineffective and highly toxic[52]. Therefore, targeted therapies against PDAC are urgently needed. L48H37, a stable curcumin analog, inhibits lung cancer cell growth and induce apoptosis *in vitro* and *in vivo*. Its mechanism of action includes increased production of ROS, activation of the ER stress pathway and inhibition of STAT3 phosphorylation[30]. In addition, L48H37 triggers the release of mitochondrial cytochrome c, and activates caspase-9, caspase-8 and caspase-3 to induce the apoptotic pathway[53]. L48H37 treatment significantly increased ROS levels in PDAC cells, which resulted in loss of MMP. L48H37 also promoted Bax elevation and decreased Bcl-2 in a dose-dependent manner during apoptosis initiation, and blocked the cell cycle at the G2/M phase. Taken together, L48H37 inhibits PDAC cell growth *via* multiple targets and pathways.

Pancreatic cancer is driven by both genetic and epigenetic aberrations, especially in histone-modifier genes, which have been associated with tumor progression and chemo-resistance[54-56]. L48H37 downregulated the histone methyltransferase KMT2D, which in turn augmented L48H37-induced apoptosis and blocked migration. KMT2D is an essential epigenetic modifier containing highly conserved SET domains, and catalyzes the monomethylation of lysine at position 4 of histone H3 (H3K4). In addition, L48H37 also downregulated H3K4me1, an epigenetic marker of the active transcription of genes associated with tumorigenic pathways[3,57]. However, the function of KMT2D in the tumor is highly complex, with some studies showing a tumor suppressing and others a tumor promoting function. For example, KMT2D upregulated p53 in cancer cells following doxorubicin-induced DNA damage[58], while KMT2D inhibition increased aerobic glycolysis in tumor cells and altered the lipidomic profiles mediated by the glucose transporter SLC2A3, resulting in increased tumor growth[28]. On the other hand, the overexpression of KMT2D in ER-positive breast cancer cells increased the recruitment and activation of FOXA1, PBX1 and ER, which limited the efficacy of PI3K inhibitors[23]. KMT2D deficiency has also been

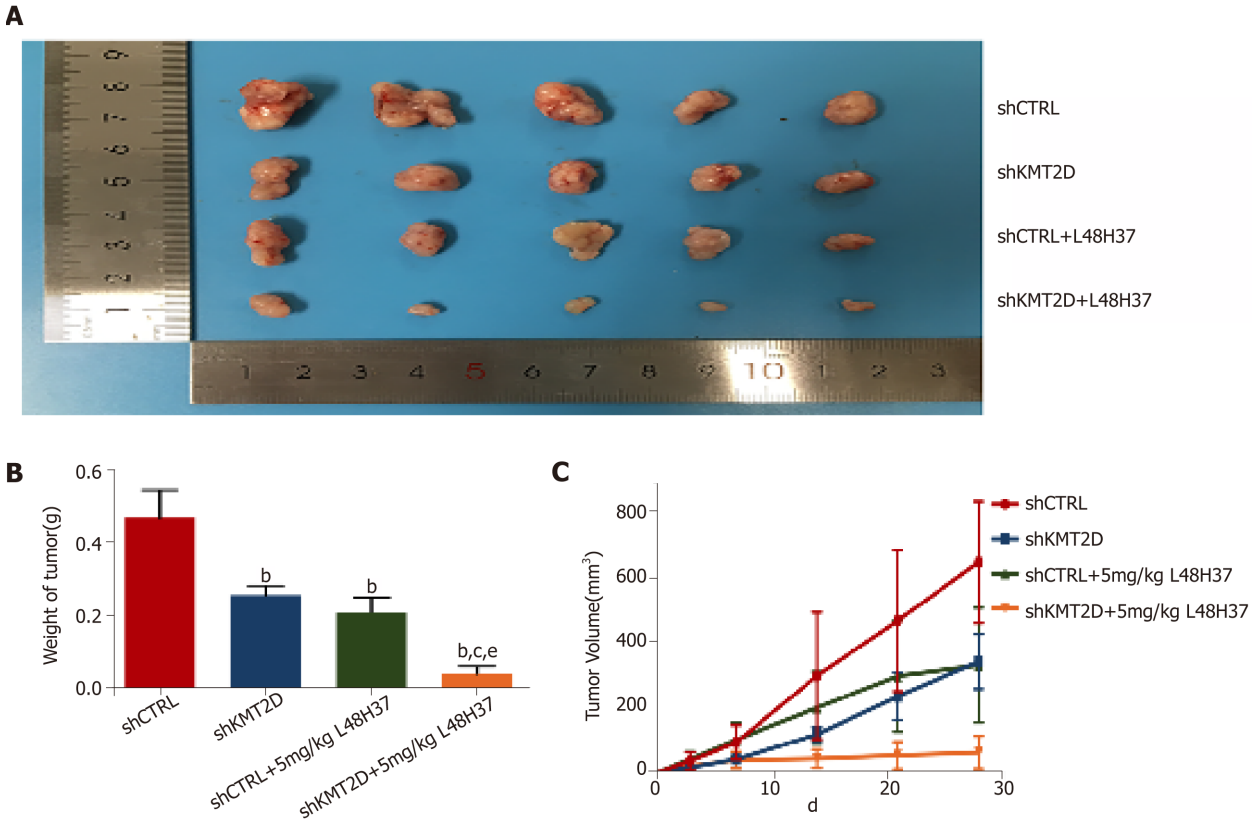

Figure 6 KMT2D knockdown synergizes with L48H37 to inhibit pancreatic ductal adenocarcinoma xenograft growth *in vivo*. A: The gross image of resected tumors; B: Effect of 5 mg/kg L48H37 treatment on wet tumor weight in relatively independent four sub-groups (shCTRL group, shKMT2D group, shCTRL + 5 mg/kg L48H37 group and shKMT2D + 5 mg/kg L48H37 group). Data were expressed as mean ± SEM. $^{b}P < 0.01$ *vs* shCTRL group. $^{c}P < 0.05$ *vs* shKMT2D group. $^{e}P < 0.05$ *vs* shCTRL + 5 mg/kg L48H37 group; C: Tumor volumes recorded at different follow-up times in the above four sub-groups. Data were expressed as mean ± SEM. $P < 0.01$ (shCTRL group *vs* shKMT2D group; shCTRL group *vs* shCTRL + 5 mg/kg L48H37 group; shCTRL group *vs* shKMT2D + 5 mg/kg L48H37 group; shKMT2D group *vs* shKMT2D + 5 mg/kg L48H37 group; shCTRL + 5 mg/kg L48H37 group *vs* shKMT2D + 5 mg/kg L48H37 group).

associated with reduced proliferation and increased apoptosis in gastric[16], pancreatic[15], prostate[18] and colon[59] cancer cells. In addition, a KMT2D mutation in T-lymphoma cells increased their sensitivity to the histone deacetylase inhibitor chidamide, in combination with the hypo-methylating agent decitabine, by modulating the KMT2D/H3K4me axis[60]. Based on our and others' findings, we hypothesize that KMT2D has a tumor type- and stage-specific role, and can be manipulated to limit tumor growth and enhance chemotherapeutic effects.

KMT2D knockdown further activated the PERK/eIF2a/ATF4/CHOP ER stress pathway in PDAC cells in the presence of L48H37. This is the first study to link KMT2D with ER stress-induced apoptosis. ER stress activates the unfolded protein response (UPR) *via* IRE1α, PERK/ATF4 and ATF6, which eventually leads to cell death[61]. Due to higher translation rates in cancer cells, they are more susceptible to the generation and accumulation of misfolded proteins, which triggers ER stress, UPR and apoptosis[62]. Previous studies showed a link between histone methyltransferase and ER stress. The euchromatin histone-lysine N-methyltransferase 2 (EZH2) inhibitor sensitizes breast cancer cells to TRAIL by upregulating ATF4/CHOP-dependent DR5 expression in a ROS-dependent manner[51]. EZH2 inhibitors also reverse the high levels of histone 3 lysine 27 trimethylation on the IRE1 promoter, which restores IRE1 expression and impairs tumor growth[63]. The histone lysine demethylase KDM4C activates ATF4 transcription, and reprograms amino acid metabolism for cancer cell proliferation[64]. Inhibition of eukaryotic histone methyltransferase G9a by BIX01294 downregulates MCL1 and suppresses proliferation in lung and bladder cancer cells[65]. Deficiency of MLL1, a homologue of KMT2D, enhances tunicamycin-induced UPR and apoptosis[66]. Nevertheless, the specific interaction between methyltransferases and the ER stress pathway requires further study.

Bioinformatics analysis of the RNA Seq data of KMT2D knockdown PDAC cell lines revealed elevated expression of genes involved in the regulation of extrinsic apoptotic signaling pathways, including PPP2R1B, IL1A, MAPK8IP2, MCL1, ELL3, PDCD6, HIC1 and PTPMT1. Downregulation of PPP2R1B increases AKT

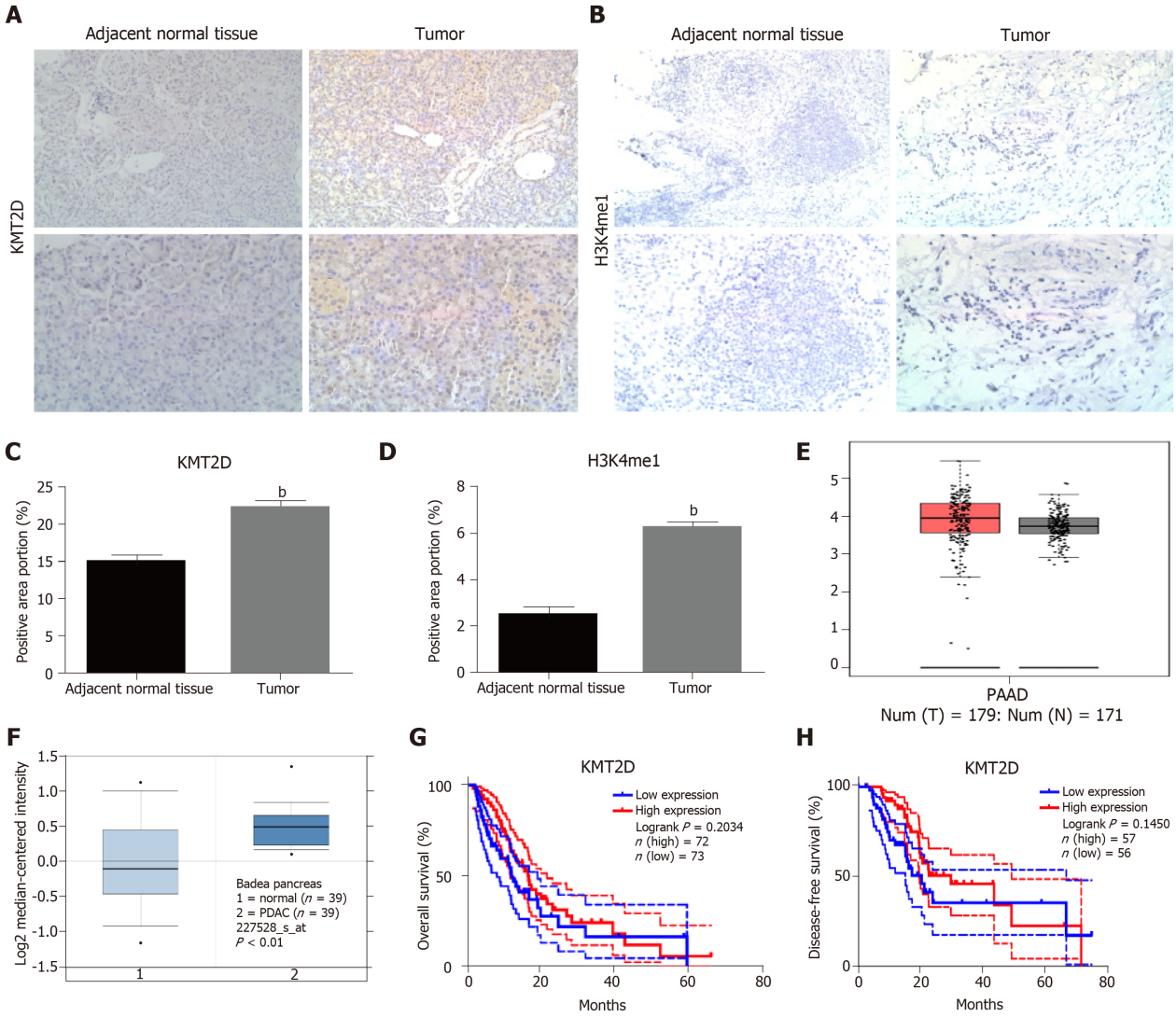

Figure 7 The prognostic value of the KMT2D in pancreatic ductal adenocarcinoma. A-D: Representative immunohistochemistry images showing KMT2D or H3K4me1 expression in PDAC tissues and paired normal tissues (200× and 400× magnification). The histogram shows the percentage of positively-stained area as calculated by Fiji. Data were expressed as mean ± SEM. $^{b}P < 0.01$ *vs* shCTRL group; E, F: Box-plot graph showing KMT2D expression in tumor and normal tissues from GEPIA and Oncomine databases; G, H: Kaplan-Meier curves showing overall survival and disease-free survival of TCGA database patients based on KMT2D expression.

phosphorylation and 5-FU resistance in colorectal cancer, and restoring PPP2R1B sensitizes the cells to 5-FU-induced apoptosis[67]. Unlike secretory IL-1α, which promotes tumor growth, surface IL-1α enables adhesion of tumor cells to immune effector cells and blocks tumor invasion[68]. Higher expression of MAPK8IP2 was significantly associated with improved overall survival (but not disease-free survival, data not shown) in the TCGA cohort, and was reportedly increased in malignant mesothelioma following treatment with quercetin and cisplatin[69]. MCL1 is usually highly expressed in tumor cells, and blocking it rapidly induced apoptosis and reduced drug resistance[70]. ELL3 stabilizes p53 expression in breast cancer cells and induces chemo-sensitivity *via* the ERK1/2 pathway[71]. However, it is also known to initiate anti-5-FU resistance by activating the Wnt pathway[72]. HIC1 and PDCD6 induce apoptosis in a p53-dependent manner in response to DNA damage[73-75]. PTPMT1 is involved in cancer cell metabolism, and sub-lethal downregulation with low-dose paclitaxel synergistically promotes cancer cell death[76]. Interestingly, alternative splicing to PTPMT1B instead of PTPMT1A sensitizes cancer cells to radiotherapy[77]. However, the precise roles of these molecules in pancreatic cancer need to be further explored.

In clinical PDAC specimens, we found significantly higher KMT2D mRNA and protein levels in cancer tissues compared to adjacent normal tissues, with a concomitant increase in H3K4me1, indicating that the expression and catalytic activity of KMT2D were consistent. A recent study[28] showed low levels of KMT2D in the pancreatic cancer tissues, indicating that KMT2D expression varies according to

tumor staging and sample heterogeneity, and therefore needs to be validated in larger cohorts consisting of samples from different stages. In addition, KMT2D mRNA levels were not correlated to the degree of DNA methylation (Supplement Figure 4B), but weakly associated with the methylation degree of specific sites (*e.g.*, cg229610; cor = -0.301, $P < 0.01$, Supplement Figure 4C), which may act as an alternative mechanism for KMT2D transcription. Previous studies have shown that more than half of pancreatic cancer patients with inherited KMT2 mutations have a significantly higher median survival duration compared to wild-type patients (32 mo *vs* 15.3 mo, $P = 0.0063$), while low levels of KMT2D was independently associated with better overall survival (19.9 mo *vs* 11.8 mo, log-rank $P = 0.001$). However, other studies show contrasting results[13,15,28]. Based on patient data from the TCGA database, there was no significant relationship between KMT2D expression and overall or disease-free survival,but higher KMT2D expression was found to be associated with poor tumor grading in clinical and pathological analyses. These discrepancies could be the result of different stratification criteria and treatment regimens, and require further studies for clarification.

In conclusion, KMT2D deficiency enhances the therapeutic effects of L48H37 against PDAC. Our findings provide new insights into targeting histone methyltransferases in combination with chemotherapy in order to improve efficacy of the latter.

ARTICLE HIGHLIGHTS

Research background

Pancreatic ductal adenocarcinoma is a kind of refractory disease with high mortality. Novel therapeutic strategies are urgently needed for patients with advanced pancreatic cancer.

Research motivation

Recent findings showed the predictive and therapeutic value of targeting lysine methylation signaling in pancreatic ductal adenocarcinoma (PDAC). L48H37, a novel curcumin analog, which potentially acts on histone-lysine N-methyltransferase 2D. The relationship between these two factors in the treatment of pancreatic cancer remains unknown, and the answer to this question gives significant insight into the additional ways in which these interventions work and may improve treatment efficacy.

Research objectives

To determine the anti-cancer effect of L48H37 alone and combined with KMT2D deficiency in PDAC. L48H37 turned out to have better efficacy in anti-pancreatic cancer in the absence of KMT2D. Targeting histone methyltransferase in combination with chemotherapy provides a new direction for cancer treatment.

Research methods

In vitro, the viability and proliferation of PDAC cell lines were determined by CCK8 and colony formation assay. Apoptosis, mitochondrial membrane potential (MMP), reactive oxygen species (ROS) levels and cell cycle profile were investigated by flow cytometry methods. Migration was assessed by the wound healing assay. The protein and mRNA levels of relevant factors in cells or tissues were analyzed by immunologic- and molecular-based assays. *In vivo* tumor xenografts were also established. In addition, a bioinformatics prediction was run throughout this entire study.

Research results

L48H37 inhibited proliferation and induced apoptosis in SW1990 and ASPC-1 cells in a dose- and time-dependent manner, while also reducing MMP, increasing ROS levels, arresting cell cycle at the G2/M stages and activating the ER stress pathway. Silencing KMT2D significantly augmented L48H37-induced apoptosis and the ER stress pathway. Targeting KMT2D in combination with L48H37 remarkably reduced tumor loading in nude mice. The differentially expressed genes in KMT2D-deficient PDAC cell lines were functionally categorized into the extrinsic apoptotic signaling pathway. However, in contrast to other research, there is no evidence that KMT2D expression level is related to prognosis. The key target of KMT2D deficiency for treatment remains to be studied.

Research conclusions

We report here for the first time that L48H37 exerts a potent anti-cancer effect in PDAC, which is augmented by KMT2D deficiency. These results pave the way for the combined application of targeting epigenetic therapy and chemotherapy.

Research perspectives

Our findings provide new insights into targeting histone methyltransferases in combination with chemotherapy in order to improve the efficacy of the latter.

REFERENCES

1 **Neoptolemos JP**, Kleeff J, Michl P, Costello E, Greenhalf W, Palmer DH. Therapeutic developments in pancreatic cancer: current and future perspectives. *Nat Rev Gastroenterol Hepatol* 2018; **15**: 333-348 [PMID: 29717230 DOI: 10.1038/s41575-018-0005-x]

2 **Bögershausen N**, Bruford E, Wollnik B. Skirting the pitfalls: a clear-cut nomenclature for H3K4 methyltransferases. *Clin Genet* 2013; **83**: 212-214 [PMID: 23130995 DOI: 10.1111/cge.12050]

3 **Froimchuk E**, Jang Y, Ge K. Histone H3 lysine 4 methyltransferase KMT2D. *Gene* 2017; **627**: 337-342 [PMID: 28669924 DOI: 10.1016/j.gene.2017.06.056]

4 **Papke DJ**, Nowak JA, Yurgelun MB, Frieden A, Srivastava A, Lindeman NI, Sholl LM, MacConaill LE, Dong F. Validation of a targeted next-generation sequencing approach to detect mismatch repair deficiency in colorectal adenocarcinoma. *Mod Pathol* 2018; **31**: 1882-1890 [PMID: 29955144 DOI: 10.1038/s41379-018-0091-x]

5 **Salem ME**, Puccini A, Xiu J, Raghavan D, Lenz HJ, Korn WM, Shields AF, Philip PA, Marshall JL, Goldberg RM. Comparative Molecular Analyses of Esophageal Squamous Cell Carcinoma, Esophageal Adenocarcinoma, and Gastric Adenocarcinoma. *Oncologist* 2018; **23**: 1319-1327 [PMID: 29866946 DOI: 10.1634/theoncologist.2018-0143]

6 **Yap YS**, Munusamy P, Lim C, Chan CHT, Prawira A, Loke SY, Lim SH, Ong KW, Yong WS, Ng SBH, Tan IBH, Callen DF, Lim JCT, Thike AA, Tan PH, Lee ASG. Breast cancer in women with neurofibromatosis type 1 (NF1): a comprehensive case series with molecular insights into its aggressive phenotype. *Breast Cancer Res Treat* 2018; **171**: 719-735 [PMID: 29926297 DOI: 10.1007/s10549-018-4851-6]

7 **Lucchesi C**, Khalifa E, Laizet Y, Soubeyran I, Mathoulin-Pelissier S, Chomienne C, Italiano A. Targetable Alterations in Adult Patients With Soft-Tissue Sarcomas: Insights for Personalized Therapy. *JAMA Oncol* 2018; **4**: 1398-1404 [PMID: 29801054 DOI: 10.1001/jamaoncol.2018.0723]

8 **Van Every MJ**, Dancik G, Paramesh V, Gurda GT, Meier DR, Cash SE, Richmond CS, Guin S. Genomic case report of a low grade bladder tumor metastasis to lung. *BMC Urol* 2018; **18**: 74 [PMID: 30176882 DOI: 10.1186/s12894-018-0386-8]

9 **Sasanakietkul T**, Murtha TD, Javid M, Korah R, Carling T. Epigenetic modifications in poorly differentiated and anaplastic thyroid cancer. *Mol Cell Endocrinol* 2018; **469**: 23-37 [PMID: 28552796 DOI: 10.1016/j.mce.2017.05.022]

10 **Ardeshir-Larijani F**, Bhateja P, Lipka MB, Sharma N, Fu P, Dowlati A. KMT2D Mutation Is Associated With Poor Prognosis in Non-Small-Cell Lung Cancer. *Clin Lung Cancer* 2018; **19**: e489-e501 [PMID: 29627316 DOI: 10.1016/j.cllc.2018.03.005]

11 **Hillman RT**, Celestino J, Terranova C, Beird HC, Gumbs C, Little L, Nguyen T, Thornton R, Tippen S, Zhang J, Lu KH, Gershenson DM, Rai K, Broaddus RR, Futreal PA. KMT2D/MLL2 inactivation is associated with recurrence in adult-type granulosa cell tumors of the ovary. *Nat Commun* 2018; **9**: 2496 [PMID: 29950560 DOI: 10.1038/s41467-018-04950-x]

12 **Soulières D**, Licitra L, Mesía R, Remenár É, Li SH, Karpenko A, Chol M, Wang YA, Solovieff N, Bourdeau L, Sellami D, Faivre S. Molecular Alterations and Buparlisib Efficacy in Patients with Squamous Cell Carcinoma of the Head and Neck: Biomarker Analysis from BERIL-1. *Clin Cancer Res* 2018; **24**: 2505-2516 [PMID: 29490986 DOI: 10.1158/1078-0432.CCR-17-2644]

13 **Sausen M**, Phallen J, Adleff V, Jones S, Leary RJ, Barrett MT, Anagnostou V, Parpart-Li S, Murphy D, Kay Li Q, Hruban CA, Scharpf R, White JR, O'Dwyer PJ, Allen PJ, Eshleman JR, Thompson CB, Klimstra DS, Linehan DC, Maitra A, Hruban RH, Diaz LA, Von Hoff DD, Johansen JS, Drebin JA, Velculescu VE. Clinical implications of genomic alterations in the tumour and circulation of pancreatic cancer patients. *Nat Commun* 2015; **6**: 7686 [PMID: 26154128 DOI: 10.1038/ncomms8686]

14 **Gleeson FC**, Kerr SE, Kipp BR, Voss JS, Minot DM, Tu ZJ, Henry MR, Graham RP, Vasmatzis G, Cheville JC, Lazaridis KN, Levy MJ. Targeted next generation sequencing of endoscopic ultrasound acquired cytology from ampullary and pancreatic adenocarcinoma has the potential to aid patient stratification for optimal therapy selection. *Oncotarget* 2016; **7**: 54526-54536 [PMID: 27203738 DOI: 10.18632/oncotarget.9440]

15 **Dawkins JB**, Wang J, Maniati E, Heward JA, Koniali L, Kocher HM, Martin SA, Chelala C, Balkwill FR, Fitzgibbon J, Grose RP. Reduced Expression of Histone Methyltransferases KMT2C and KMT2D Correlates with Improved Outcome in Pancreatic Ductal Adenocarcinoma. *Cancer Res* 2016; **76**: 4861-4871 [PMID: 27280393 DOI: 10.1158/0008-5472.CAN-16-0481]

16 **Xiong W**, Deng Z, Tang Y, Deng Z, Li M. Downregulation of KMT2D suppresses proliferation and induces apoptosis of gastric cancer. *Biochem Biophys Res Commun* 2018; **504**: 129-136 [PMID: 30177394 DOI: 10.1016/j.bbrc.2018.08.143]

17 **Abudureheman A**, Ainiwaer J, Hou Z, Niyaz M, Turghun A, Hasim A, Zhang H, Lu X, Sheyhidin I. High MLL2 expression predicts poor prognosis and promotes tumor progression by inducing EMT in esophageal squamous cell carcinoma. *J Cancer Res Clin Oncol* 2018; **144**: 1025-1035 [PMID: 29532228 DOI: 10.1007/s00432-018-2625-5]

18 **Lv S**, Ji L, Chen B, Liu S, Lei C, Liu X, Qi X, Wang Y, Lai-Han Leung E, Wang H, Zhang L, Yu X, Liu Z, Wei Q, Lu L. Histone methyltransferase KMT2D sustains prostate carcinogenesis and metastasis via epigenetically activating LIFR and KLF4. *Oncogene* 2018; **37**: 1354-1368 [PMID: 29269867 DOI: 10.1038/s41388-017-0026-x]

19 **Dhar SS**, Zhao D, Lin T, Gu B, Pal K, Wu SJ, Alam H, Lv J, Yun K, Gopalakrishnan V, Flores ER, Northcott PA, Rajaram V, Li W, Shilatifard A, Sillitoe RV, Chen K, Lee MG. MLL4 Is Required to Maintain Broad H3K4me3 Peaks and Super-Enhancers at Tumor Suppressor Genes. *Mol Cell* 2018; **70**: 825-841.e6 [PMID: 29861161 DOI: 10.1016/j.molcel.2018.04.028]

20 **Kalu NN**, Mazumdar T, Peng S, Tong P, Shen L, Wang J, Banerjee U, Myers JN, Pickering CR, Brunell D, Stephan CC, Johnson FM. Comprehensive pharmacogenomic profiling of human papillomavirus-positive and -negative squamous cell carcinoma identifies sensitivity to aurora kinase inhibition in KMT2D mutants. *Cancer Lett* 2018; **431**: 64-72 [PMID: 29807113 DOI: 10.1016/j.canlet.2018.05.029]

21 **Koren S**, Bentires-Alj M. Tackling Resistance to PI3K Inhibition by Targeting the Epigenome. *Cancer Cell* 2017; **31**: 616-618 [PMID: 28486103 DOI: 10.1016/j.ccell.2017.04.010]

22 **Ganesh K**, Shah RH, Vakiani E, Nash GM, Skottowe HP, Yaeger R, Cercek A, Lincoln A, Tran C, Segal NH, Reidy DL, Varghese A, Epstein AS, Sonoda Y, Chi D, Guillem J, Temple L, Paty P, Hechtman J, Shia J, Weiser M, Aguilar JG, Kemeny N, Berger MF, Saltz L, Stadler ZK. Clinical and genetic determinants of ovarian metastases from colorectal cancer. *Cancer* 2017; **123**: 1134-1143 [PMID:

27875625 DOI: 10.1002/cncr.30424]
23 **Toska E**, Osmanbeyoglu HU, Castel P, Chan C, Hendrickson RC, Elkabets M, Dickler MN, Scaltriti M, Leslie CS, Armstrong SA, Baselga J. PI3K pathway regulates ER-dependent transcription in breast cancer through the epigenetic regulator KMT2D. *Science* 2017; **355**: 1324-1330 [PMID: 28336670 DOI: 10.1126/science.aah6893]
24 **Simbolo M**, Mafficini A, Sikora KO, Fassan M, Barbi S, Corbo V, Mastracci L, Rusev B, Grillo F, Vicentini C, Ferrara R, Pilotto S, Davini F, Pelosi G, Lawlor RT, Chilosi M, Tortora G, Bria E, Fontanini G, Volante M, Scarpa A. Lung neuroendocrine tumours: deep sequencing of the four World Health Organization histotypes reveals chromatin-remodelling genes as major players and a prognostic role for TERT, RB1, MEN1 and KMT2D. *J Pathol* 2017; **241**: 488-500 [PMID: 27873319 DOI: 10.1002/path.4853]
25 **Albrecht D**, Ceschin J, Dompierre J, Gueniot F, Pinson B, Daignan-Fornier B. Chemo-Genetic Interactions Between Histone Modification and the Antiproliferation Drug AICAR Are Conserved in Yeast and Humans. *Genetics* 2016; **204**: 1447-1460 [PMID: 27707786 DOI: 10.1534/genetics.116.192518]
26 **Bossi D**, Cicalese A, Dellino GI, Luzi L, Riva L, D'Alesio C, Diaferia GR, Carugo A, Cavallaro E, Piccioni R, Barberis M, Mazzarol G, Testori A, Punzi S, Pallavicini I, Tosti G, Giacó L, Melloni G, Heffernan TP, Natoli G, Draetta GF, Minucci S, Pelicci P, Lanfrancone L. In Vivo Genetic Screens of Patient-Derived Tumors Revealed Unexpected Frailty of the Transformed Phenotype. *Cancer Discov* 2016; **6**: 650-663 [PMID: 27179036 DOI: 10.1158/2159-8290.CD-15-1200]
27 **Kim JH**, Sharma A, Dhar SS, Lee SH, Gu B, Chan CH, Lin HK, Lee MG. UTX and MLL4 coordinately regulate transcriptional programs for cell proliferation and invasiveness in breast cancer cells. *Cancer Res* 2014; **74**: 1705-1717 [PMID: 24491801 DOI: 10.1158/0008-5472.CAN-13-1896]
28 **Koutsioumpa M**, Hatziapostolou M, Polytarchou C, Tolosa EJ, Almada LL, Mahurkar-Joshi S, Williams J, Tirado-Rodriguez AB, Huerta-Yepez S, Karavias D, Kourea H, Poultsides GA, Struhl K, Dawson DW, Donahue TR, Fernández-Zapico ME, Iliopoulos D. Lysine methyltransferase 2D regulates pancreatic carcinogenesis through metabolic reprogramming. *Gut* 2018; **pii**: gutjnl-2017-315690 [PMID: 30337373 DOI: 10.1136/gutjnl-2017-315690]
29 **Dawkins JBN**. *Aberrant downstream mechanisms following depletion of KMT2C and KMT2D in Pancreatic Ductal Adenocarcinoma. Queen Mary, University of London* 2017; Available from: https://qmro.qmul.ac.uk/xmlui/bitstream/handle/123456789/24591/Dawkins_J_PhD_200317.pdf?sequence=1
30 **Feng C**, Xia Y, Zou P, Shen M, Hu J, Ying S, Pan J, Liu Z, Dai X, Zhuge W, Liang G, Ruan Y. Curcumin analog L48H37 induces apoptosis through ROS-mediated endoplasmic reticulum stress and STAT3 pathways in human lung cancer cells. *Mol Carcinog* 2017; **56**: 1765-1777 [PMID: 28218464 DOI: 10.1002/mc.22633]
31 **Abi-Habib RJ**, Singh R, Liu S, Bugge TH, Leppla SH, Frankel AE. A urokinase-activated recombinant anthrax toxin is selectively cytotoxic to many human tumor cell types. *Mol Cancer Ther* 2006; **5**: 2556-2562 [PMID: 17041100 DOI: 10.1158/1535-7163.MCT-06-0315]
32 **Li CG**, Pu MF, Li CZ, Gao M, Liu MX, Yu CZ, Yan H, Peng C, Zhao Y, Li Y, Ma ZL, Qi XM, Wang YZ, Miao LL, Ren J. MicroRNA-1304 suppresses human non-small cell lung cancer cell growth in vitro by targeting heme oxygenase-1. *Acta Pharmacol Sin* 2017; **38**: 110-119 [PMID: 27641735 DOI: 10.1038/aps.2016.92]
33 **Nolan T**, Hands RE, Bustin SA. Quantification of mRNA using real-time RT-PCR. *Nat Protoc* 2006; **1**: 1559-1582 [PMID: 17406449 DOI: 10.1038/nprot.2006.236]
34 **Masuda M**, Senju S, Fujii Si S, Terasaki Y, Takeya M, Hashimoto Si S, Matsushima K, Yumoto E, Nishimura Y. Identification and immunocytochemical analysis of DCNP1, a dendritic cell-associated nuclear protein. *Biochem Biophys Res Commun* 2002; **290**: 1022-1029 [PMID: 11798177 DOI: 10.1006/bbrc.2001.6202]
35 **Liao W**, Nguyen MT, Imamura T, Singer O, Verma IM, Olefsky JM. Lentiviral short hairpin ribonucleic acid-mediated knockdown of GLUT4 in 3T3-L1 adipocytes. *Endocrinology* 2006; **147**: 2245-2252 [PMID: 16497797 DOI: 10.1210/en.2005-1638]
36 **Edgar R**, Lash A. Chapter 6 The Gene Expression Omnibus (GEO): A Gene Expression and Hybridization Repository. Available from: https://www.ncbi.nlm.nih.gov/books/NBK21093/
37 **Mi B**, Liu G, Zhou W, Lv H, Liu Y, Liu J. Identification of genes and pathways in the synovia of women with osteoarthritis by bioinformatics analysis. *Mol Med Rep* 2018; **17**: 4467-4473 [PMID: 29344651 DOI: 10.3892/mmr.2018.8429]
38 **Cunningham CB**, Ji L, Wiberg RA, Shelton J, McKinney EC, Parker DJ, Meagher RB, Benowitz KM, Roy-Zokan EM, Ritchie MG, Brown SJ, Schmitz RJ, Moore AJ. The Genome and Methylome of a Beetle with Complex Social Behavior, Nicrophorus vespilloides (Coleoptera: Silphidae). *Genome Biol Evol* 2015; **7**: 3383-3396 [PMID: 26454014 DOI: 10.1093/gbe/evv194]
39 **Tripathi S**, Pohl MO, Zhou Y, Rodriguez-Frandsen A, Wang G, Stein DA, Moulton HM, DeJesus P, Che J, Mulder LC, Yángüez E, Andenmatten D, Pache L, Manicassamy B, Albrecht RA, Gonzalez MG, Nguyen Q, Brass A, Elledge S, White M, Shapira S, Hacohen N, Karlas A, Meyer TF, Shales M, Gatorano A, Johnson JR, Jang G, Johnson T, Verschueren E, Sanders D, Krogan N, Shaw M, König R, Stertz S, García-Sastre A, Chanda SK. Meta- and Orthogonal Integration of Influenza "OMICs" Data Defines a Role for UBR4 in Virus Budding. *Cell Host Microbe* 2015; **18**: 723-735 [PMID: 26651948 DOI: 10.1016/j.chom.2015.11.002]
40 **Tang Z**, Li C, Kang B, Gao G, Li C, Zhang Z. GEPIA: a web server for cancer and normal gene expression profiling and interactive analyses. *Nucleic Acids Res* 2017; **45**: W98-W102 [PMID: 28407145 DOI: 10.1093/nar/gkx247]
41 **Rhodes DR**, Yu J, Shanker K, Deshpande N, Varambally R, Ghosh D, Barrette T, Pandey A, Chinnaiyan AM. ONCOMINE: a cancer microarray database and integrated data-mining platform. *Neoplasia* 2004; **6**: 1-6 [PMID: 15068665 DOI: 10.1016/S1476-5586(04)80047-2]
42 **Karaayvaz M**, Zhang C, Liang S, Shroyer KR, Ju J. Prognostic significance of miR-205 in endometrial cancer. *PLoS One* 2012; **7**: e35158 [PMID: 22514717 DOI: 10.1371/journal.pone.0035158]
43 **Nohata N**, Sone Y, Hanazawa T, Fuse M, Kikkawa N, Yoshino H, Chiyomaru T, Kawakami K, Enokida H, Nakagawa M, Shozu M, Okamoto Y, Seki N. miR-1 as a tumor suppressive microRNA targeting TAGLN2 in head and neck squamous cell carcinoma. *Oncotarget* 2011; **2**: 29-42 [PMID: 21378409 DOI: 10.18632/oncotarget.213]
44 **Tang JY**, Farooqi AA, Ou-Yang F, Hou MF, Huang HW, Wang HR, Li KT, Fayyaz S, Shu CW, Chang

HW. Oxidative stress-modulating drugs have preferential anticancer effects - involving the regulation of apoptosis, DNA damage, endoplasmic reticulum stress, autophagy, metabolism, and migration. *Semin Cancer Biol* 2018 [PMID: 30149066 DOI: 10.1016/j.semcancer.2018.08.010]

45 **Han J**, Back SH, Hur J, Lin YH, Gildersleeve R, Shan J, Yuan CL, Krokowski D, Wang S, Hatzoglou M, Kilberg MS, Sartor MA, Kaufman RJ. ER-stress-induced transcriptional regulation increases protein synthesis leading to cell death. *Nat Cell Biol* 2013; **15**: 481-490 [PMID: 23624402 DOI: 10.1038/ncb2738]

46 **Gorman AM**, Healy SJ, Jäger R, Samali A. Stress management at the ER: regulators of ER stress-induced apoptosis. *Pharmacol Ther* 2012; **134**: 306-316 [PMID: 22387231 DOI: 10.1016/j.pharmthera.2012.02.003]

47 **Roth GS**, Casanova AG, Lemonnier N, Reynoird N. Lysine methylation signaling in pancreatic cancer. *Curr Opin Oncol* 2018; **30**: 30-37 [PMID: 29076964 DOI: 10.1097/CCO.0000000000000421]

48 **Roidl D**, Hellbach N, Bovio PP, Villarreal A, Heidrich S, Nestel S, Grüning BA, Boenisch U, Vogel T. DOT1L Activity Promotes Proliferation and Protects Cortical Neural Stem Cells from Activation of ATF4-DDIT3-Mediated ER Stress In Vitro. *Stem Cells* 2016; **34**: 233-245 [PMID: 26299268 DOI: 10.1002/stem.2187]

49 **Batista IAA**, Helguero LA. Biological processes and signal transduction pathways regulated by the protein methyltransferase SETD7 and their significance in cancer. *Signal Transduct Target Ther* 2018; **3**: 19 [PMID: 30013796 DOI: 10.1038/s41392-018-0017-6]

50 **Xiao D**, Wang H, Hao L, Guo X, Ma X, Qian Y, Chen H, Ma J, Zhang J, Sheng W, Shou W, Huang G, Ma D. The roles of SMYD4 in epigenetic regulation of cardiac development in zebrafish. *PLoS Genet* 2018; **14**: e1007578 [PMID: 30110327 DOI: 10.1371/journal.pgen.1007578]

51 **Kim SY**, Hong M, Heo SH, Park S, Kwon TK, Sung YH, Oh Y, Lee S, Yi GS, Kim I. Inhibition of euchromatin histone-lysine N-methyltransferase 2 sensitizes breast cancer cells to tumor necrosis factor-related apoptosis-inducing ligand through reactive oxygen species-mediated activating transcription factor 4-C/EBP homologous protein-death receptor 5 pathway activation. *Mol Carcinog* 2018; **57**: 1492-1506 [PMID: 29964331 DOI: 10.1002/mc.22872]

52 **Wang Y**, Camateros P, Cheung WY. A Real-World Comparison of FOLFIRINOX, Gemcitabine Plus nab-Paclitaxel, and Gemcitabine in Advanced Pancreatic Cancers. *J Gastrointest Cancer* 2019; **50**: 62-68 [PMID: 29143916 DOI: 10.1007/s12029-017-0028-5]

53 **Pan J**, Xu G, Yeung SC. Cytochrome c release is upstream to activation of caspase-9, caspase-8, and caspase-3 in the enhanced apoptosis of anaplastic thyroid cancer cells induced by manumycin and paclitaxel. *J Clin Endocrinol Metab* 2001; **86**: 4731-4740 [PMID: 11600533 DOI: 10.1210/jcem.86.10.7860]

54 **Ford DJ**, Dingwall AK. The cancer COMPASS: navigating the functions of MLL complexes in cancer. *Cancer Genet* 2015; **208**: 178-191 [PMID: 25794446 DOI: 10.1016/j.cancergen.2015.01.005]

55 **Paradise BD**, Barham W, Fernandez-Zapico ME. Targeting Epigenetic Aberrations in Pancreatic Cancer, a New Path to Improve Patient Outcomes? *Cancers (Basel)* 2018; **10**: pii: E128 [PMID: 29710783 DOI: 10.3390/cancers10050128]

56 **Rao RC**, Dou Y. Hijacked in cancer: the KMT2 (MLL) family of methyltransferases. *Nat Rev Cancer* 2015; **15**: 334-346 [PMID: 25998713 DOI: 10.1038/nrc3929]

57 **Jia J**, Parikh H, Xiao W, Hoskins JW, Pflicke H, Liu X, Collins I, Zhou W, Wang Z, Powell J, Thorgeirsson SS, Rudloff U, Petersen GM, Amundadottir LT. An integrated transcriptome and epigenome analysis identifies a novel candidate gene for pancreatic cancer. *BMC Med Genomics* 2013; **6**: 33 [PMID: 24053169 DOI: 10.1186/1755-8794-6-33]

58 **Lee J**, Kim DH, Lee S, Yang QH, Lee DK, Lee SK, Roeder RG, Lee JW. A tumor suppressive coactivator complex of p53 containing ASC-2 and histone H3-lysine-4 methyltransferase MLL3 or its paralogue MLL4. *Proc Natl Acad Sci USA* 2009; **106**: 8513-8518 [PMID: 19433796 DOI: 10.1073/pnas.0902873106]

59 **Guo C**, Chen LH, Huang Y, Chang CC, Wang P, Pirozzi CJ, Qin X, Bao X, Greer PK, McLendon RE, Yan H, Keir ST, Bigner DD, He Y. KMT2D maintains neoplastic cell proliferation and global histone H3 lysine 4 monomethylation. *Oncotarget* 2013; **4**: 2144-2153 [PMID: 24240169 DOI: 10.18632/oncotarget.1555]

60 **Ji MM**, Huang YH, Huang JY, Wang ZF, Fu D, Liu H, Liu F, Leboeuf C, Wang L, Ye J, Lu YM, Janin A, Cheng S, Zhao WL. Histone modifier gene mutations in peripheral T-cell lymphoma not otherwise specified. *Haematologica* 2018; **103**: 679-687 [PMID: 29305415 DOI: 10.3324/haematol.2017.182444]

61 **Chien W**, Ding LW, Sun QY, Torres-Fernandez LA, Tan SZ, Xiao J, Lim SL, Garg M, Lee KL, Kitajima S, Takao S, Leong WZ, Sun H, Tokatly I, Poellinger L, Gery S, Koeffler PH. Selective inhibition of unfolded protein response induces apoptosis in pancreatic cancer cells. *Oncotarget* 2014; **5**: 4881-4894 [PMID: 24952679 DOI: 10.18632/oncotarget.2051]

62 **Nawrocki ST**, Carew JS, Dunner K, Boise LH, Chiao PJ, Huang P, Abbruzzese JL, McConkey DJ. Bortezomib inhibits PKR-like endoplasmic reticulum (ER) kinase and induces apoptosis via ER stress in human pancreatic cancer cells. *Cancer Res* 2005; **65**: 11510-11519 [PMID: 16357160 DOI: 10.1158/0008-5472.CAN-05-2394]

63 **Bujisic B**, De Gassart A, Tallant R, Demaria O, Zaffalon L, Chelbi S, Gilliet M, Bertoni F, Martinon F. Impairment of both IRE1 expression and XBP1 activation is a hallmark of GCB DLBCL and contributes to tumor growth. *Blood* 2017; **129**: 2420-2428 [PMID: 28167662 DOI: 10.1182/blood-2016-09-741348]

64 **Zhao E**, Ding J, Xia Y, Liu M, Ye B, Choi JH, Yan C, Dong Z, Huang S, Zha Y, Yang L, Cui H, Ding HF. KDM4C and ATF4 Cooperate in Transcriptional Control of Amino Acid Metabolism. *Cell Rep* 2016; **14**: 506-519 [PMID: 26774480 DOI: 10.1016/j.celrep.2015.12.053]

65 **Cui J**, Sun W, Hao X, Wei M, Su X, Zhang Y, Su L, Liu X. EHMT2 inhibitor BIX-01294 induces apoptosis through PMAIP1-USP9X-MCL1 axis in human bladder cancer cells. *Cancer Cell Int* 2015; **15**: 4 [PMID: 25685062 DOI: 10.1186/s12935-014-0149-x]

66 **Wang X**, Ju L, Fan J, Zhu Y, Liu X, Zhu K, Wu M, Li L. Histone H3K4 methyltransferase Mll1 regulates protein glycosylation and tunicamycin-induced apoptosis through transcriptional regulation. *Biochim Biophys Acta* 2014; **1843**: 2592-2602 [PMID: 24983772 DOI: 10.1016/j.bbamcr.2014.06.013]

67 **Zhang Y**, Talmon G, Wang J. MicroRNA-587 antagonizes 5-FU-induced apoptosis and confers drug resistance by regulating PPP2R1B expression in colorectal cancer. *Cell Death Dis* 2016; **7**: e2525 [PMID: 28005075 DOI: 10.1038/cddis.2016.450]

68 **Apte RN**, Dotan S, Elkabets M, White MR, Reich E, Carmi Y, Song X, Dvozkin T, Krelin Y, Voronov E. The involvement of IL-1 in tumorigenesis, tumor invasiveness, metastasis and tumor-host interactions. *Cancer Metastasis Rev* 2006; **25**: 387-408 [PMID: 17043764 DOI: 10.1007/s10555-006-9004-4]

69 **Demiroglu-Zergeroglu A**, Ergene E, Ayvali N, Kuete V, Sivas H. Quercetin and Cisplatin combined treatment altered cell cycle and mitogen activated protein kinase expressions in malignant mesotelioma cells. *BMC Complement Altern Med* 2016; **16**: 281 [PMID: 27514524 DOI: 10.1186/s12906-016-1267-x]

70 **Akgul C**. Mcl-1 is a potential therapeutic target in multiple types of cancer. *Cell Mol Life Sci* 2009; **66**: 1326-1336 [PMID: 19099185 DOI: 10.1007/s00018-008-8637-6]

71 **Ahn HJ**, Kim KS, Shin KW, Lim KH, Kim JO, Lee JY, Kim J, Park JH, Yang KM, Baek KH, Ko JJ, Park KS. Ell3 stabilizes p53 following CDDP treatment via its effects on ubiquitin-dependent and -independent proteasomal degradation pathways in breast cancer cells. *Oncotarget* 2015; **6**: 44523-44537 [PMID: 26540344 DOI: 10.18632/oncotarget.5972]

72 **Poling A**, Sewell RG, Gallus JA, Nearchou NI. Lethality of opioid and antihistaminic combinations in mice. *Pharmacol Biochem Behav* 1985; **22**: 333-335 [PMID: 2858870 DOI: 10.3892/ol.2017.5996]

73 **Suzuki K**, Dashzeveg N, Lu ZG, Taira N, Miki Y, Yoshida K. Programmed cell death 6, a novel p53-responsive gene, targets to the nucleus in the apoptotic response to DNA damage. *Cancer Sci* 2012; **103**: 1788-1794 [PMID: 22712728 DOI: 10.1111/j.1349-7006.2012.02362.x]

74 **Chen WY**, Wang DH, Yen RC, Luo J, Gu W, Baylin SB. Tumor suppressor HIC1 directly regulates SIRT1 to modulate p53-dependent DNA-damage responses. *Cell* 2005; **123**: 437-448 [PMID: 16269335 DOI: 10.1016/j.cell.2005.08.011]

75 **Park SH**, Lee JH, Lee GB, Byun HJ, Kim BR, Park CY, Kim HB, Rho SB. PDCD6 additively cooperates with anti-cancer drugs through activation of NF-κB pathways. *Cell Signal* 2012; **24**: 726-733 [PMID: 22142513 DOI: 10.1016/j.cellsig.2011.11.006]

76 **Niemi NM**, Lanning NJ, Westrate LM, MacKeigan JP. Downregulation of the mitochondrial phosphatase PTPMT1 is sufficient to promote cancer cell death. *PLoS One* 2013; **8**: e53803 [PMID: 23326511 DOI: 10.1371/journal.pone.0053803]

77 **Sheng J**, Zhao Q, Zhao J, Zhang W, Sun Y, Qin P, Lv Y, Bai L, Yang Q, Chen L, Qi Y, Zhang G, Zhang L, Gu C, Deng X, Liu H, Meng S, Gu H, Liu Q, Coulson JM, Li X, Sun B, Wang Y. SRSF1 modulates PTPMT1 alternative splicing to regulate lung cancer cell radioresistance. *EBioMedicine* 2018; **38**: 113-126 [PMID: 30429088 DOI: 10.1016/j.ebiom.2018.11.007]

Published By Baishideng Publishing Group Inc
7041 Koll Center Parkway, Suite 160, Pleasanton, CA 94566, USA
Telephone: +1-925-2238242
Fax: +1-925-2238243
E-mail: bpgoffice@wjgnet.com
Help Desk:https://www.f6publishing.com/helpdesk
https://www.wjgnet.com